Master Thesis

Cyclic plasticity's models for thermo-mechanical applications. Case of a copper mold for continuous casting

Marco Andreola
Master in Mechanical Engineering

Udine University
Udine 2017

Cyclic plasticity's models for thermo-mechanical applications. Case of a copper mold for continuous casting

Department of Mechanical Engineering

Marco Andreola

Cyclic plasticity's models for thermo-mechanical applications. Case of a copper mold for continuous casting

Supervisors: Francesco De Bona
Jelena Srnec Novak

Title: Cyclic plasticity's models for thermo-mechanical applications. Case of a copper mold for continuous casting

Publisher: University of Udine, 2017
www.uniud.it

:

0000-0000

Abstract

This master thesis aims to investigate and to assess the fatigue life of a component that undergoes cyclic thermal loads. This study will consider different approaches through the use of different material models, providing a final comparison of the assessed fatigue life. The case study is a cylindrical copper mold used for continuous casting of steel; in order to work at high temperature the mold is properly cooled, but nevertheless high stresses arise due to the huge thermal flux and its uneven distribution.
The beginning of this work is focused on understanding theories and models available in literature in order to implement data in a finite element software. A comparison of two software (Ansys and Marc Mentat) is carried out, with the purpose of verifying experimental data coming from another work [3]. Subsequently we use Marc Mentat to define a coupled thermal-mechanical analysis, and we perform it using a combined model. A huge computational time is required to get the solution, so other models were exploited in order to save time, and the variation of the obtained solution was evaluated. Several simulations are performed for reaching stabilized conditions, from where strain data will be used to define fatigue life through the number of cycles to failure.
The subsequent chapter takes care of this last concept, giving a brief explanation of fatigue and using data coming from previous simulations for assessing fatigue life.
A final comparison is provided with the purpose of finding a trade off between the solution's reliability and the time employed. In the appendix the macro used for the computed simulations are attached.

Acknowledges

To prepare this work, I am so grateful to Prof. Francesco De Bona and PhD Jelena Srnec Novak who have helped me motivating and giving to me such useful suggestions. I'm also grateful to Almatec srl for technical support with Marc Mentat, moreover even to Roger Coianiz and Matteo Manighetti for precious advices. I thank my parents for economical support throughout the time I studied. Finally, I would like to acknowledge with gratitude, for the support and the ideas gave me, two people so important in these last years. Thank you Fabrizia. Thank you Enzo.

Contents

List of Figures

List of Tables

Nomenclature

A	Actual cross section area
A_0	Initial cross section area
$\underline{A}$	Deviatoric stress tensor
$\underline{B}$	Hydrostatic stress tensor
b	Speed of stabilization
b^*	Fatigue strength exponent or Basquin exponent
c	Fatigue ductility exponent
C	Initial plastic modulus
$d\underline{\varepsilon}$	Total strain increment tensor
E	Elastic modulus or Young's modulus
Err_{11}	Relative error percentage for strain range, committed in axial direction
Err_{22}	Relative error percentage for strain range, committed in radial direction
Err_{33}	Relative error percentage for strain range, committed in circumferential direction
Err_{eq}	Relative error percentage for equivalent strain range assessment
Es	Elastic modulus coming from stabilized conditions
F	Force applied
$f(\underline{A})$	Yield surface or yield function
G	Elastic shear modulus

$\underline{I}$	Unit tensor
K	Cyclic strength coefficient
l	Actual length
l_0	Initial length
m	Cyclic hardening exponent
N	Number of cycles
N_n	Number of cycles normalized
N_f	Number of cycles to failure
R	Isotropic hardening function
R_∞	Saturation stress
$S11$	Stress in axial direction
$S22$	Stress in radial direction
$S33$	Stress in Circumferential direction
$\underline{\alpha}$	Back stress tensor
$\Delta\varepsilon$	Total strain range
$\Delta\varepsilon_{el}$	Elastic strain range
$\Delta\varepsilon_{eq}$	Equivalent strain range
$\Delta\varepsilon_{pl}$	Plastic strain range
$\Delta\varepsilon_{rl}$	Relative error percentage committed in life assessment
$\Delta\sigma$	Stress range
Δ_{S11}	Relative error percentage for stress, committed in axial direction
Δ_{S22}	Relative error percentage for stress, committed in radial direction
Δ_{S33}	Relative error percentage for stress, committed in circumferential direction
$\varepsilon_f^{'}$	Fatigue ductility coefficient
ε_1	Total strain range in axial direction
ε_2	Total strain range in radial direction

ε_3	Total strain range in Circumferential direction
$d\underline{\varepsilon}_{el}$	Elastic strain increment tensor
$d\underline{\varepsilon}_{pl}$	Plastic strain increment tensor
$d\underline{\varepsilon}_{pl}$	Actual plasticity tensor
ε_a	Strain amplitude
ε_{el}	Elastic strain
$\varepsilon_{el,a}$	Elastic strain amplitude
ε_{eng}	Engineering strain
ε_{ij}	Element of strain tensor
ε_m	Mean strain
ε_{max}	Maximum strain
ε_{min}	Minimum strain
ε_{pl}	Plastic strain
$\varepsilon_{pl,a}$	Plastic strain amplitude
$\varepsilon_{pl,acc}$	Accumulated plastic strain
$d\varepsilon_{pl,acc}$	Accumulated plastic strain increment
ε_{pl-n}	Plastic strain range normalized
$\underline{\varepsilon}$	Strain tensor
ε_{true}	True strain
γ	Nonlinear recovery parameter or rate of stress saturation
ν	Poisson's ratio
σ	Stress value
$\underline{\sigma}$	Stress tensor
σ_{0*}	Actual yield stress
σ_{ij}	Element of the stress tensor
σ_{uts}	Ultimate tension strength
σ_a	Stress amplitude

σ_{eng}	Engineering stress
$\sigma_f^{'}$	Fatigue strength coefficient
σ_{true}	True stress
σ_{vm}	Von Mises stress or equivalent stress
σ_{y0}	Yield stress

Chapter 1
Physics of phenomena

1.1 Physical mechanism of deformation

Metals and alloys are made up of arrangements of atoms held together by electromagnetic forces between the electrons of neighbouring atoms [1].
Since is valid the principle of minimum energy conditions of the atoms packing, stable arrangements are determined and they are functions of the thermal activation. In metals, the bonds result from a sharing of electrons in the outer shells of the atoms [1]. Sometimes the structure of an alloy can belong to one of the constitutive elements or to a completely different structure; therefore, the substitution of an atom or the insertion of small atoms in the network of the solvent happens. This previous example can be employed to describe for instance respectively aluminum in iron and carbon in iron.
Metals can take different phases depending on the temperature; moreover, it is possible to distinguish the cases in which the substitute atoms occur in a disordered state or in an ordered way[1].
Generally metals are produced melting at high temperature a metal or a set of different materials. During the cooling phase the relative distances among the atoms become smaller causing, once a critical distance is reached, the growth of the first germs of a crystal. Hence from here the lattices oriented in random directions start to form. Each nucleus develops into a crystal whose growth is limited by neighbouring crystals; a poly-crystal is made up of several monocrystals oriented randomly[1].
In macroscopic scale the structure of the perfect crystal as described can represent only the elastic behavior and the brittle fracture. Nevertheless, one can see in a solid solution can be founded several defects through inserted or substituted atoms and vacancies, causing distortion of the lattice. This last sentence explains the so called point defects. Although these defects are not neglectable, the most important ones are the line defects commonly called dislocations. They are the main responsibles in the plasticity phenomena.
Dislocations arises during the growth phase of the crystal.Figure 1.1 [1] presents

an examples of dislocation.

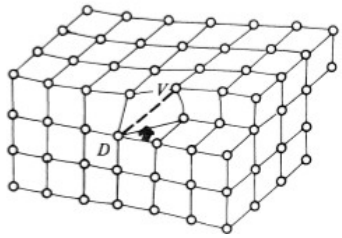

Figure 1.1: Screw dislocation.

So theory states that elastic deformations occur at the atomic level, hence the macroscopic effect is the result for balancing the external loads; however these geometrical variations are mostly reversible in fact once the load is removed the initial configuration has established again. If this phenomena doesn't happen , obviously applying a load, it means we have to deal with a plastic deformation. Even if theory has not analyzed in details, some useful concepts can be listed:

- Elastic deformation: it shows with reversible relative movement of atoms, nevertheless the elastic deformation at macroscopic scale is rather different considering the sum of micro deformations because there are irreversible crystalline slips caused by residual stresses;
- Elastic limit: known as yield stress is the threshold stress where the first irreversible movement of dislocations occurs. This is quite tricky to detect therefore it is common to assume the value linked with a permanent strain equal to 0.02 % ;
- Plastic deformation: When a stress is applied along a certain direction the slip planes are oriented, in respect to it, at $\alpha = \pi/4$. Other slip systems are triggered by reorientation of necessary crystals to ensure compatibility of deformations. This kind of deformations is permanent and stable.
- Hardening: If the stress continues to rise, the dislocation density has increased but the number of barriers is increased even more, so for this reason the deformation cannot progress unless the load is increased further[1]. This increased resistance to slip deformation is the phenomena of hardening[1].

1.1.1 Effects of monotonic loading on material behavior

In practice it's impossible to understand, for engineering applications, the material behavior using the knowledge related with lattice and its defects. Further, there are many factors not taken into account, that can influence how material behaves; some examples are temperature, residual stresses, blowholes,etc.
To overcome this drawback it is common to perform uniaxial tensile testing for measuring mechanical properties of specimens considered. This kind of test is certified and regulated by ISO 527-1, ISO 527-2, ASTM D 638 [9], here we can give a brief explanation about the procedure is given.
A tensile test machine is employed, in this machine a cylindrical specimen (with unified dimensions) is blocked through grips in order to apply a load (F) along its axis. In this way, the machine applies an increasing load and records data about extension or compression (l) undergone by the specimen and the applied force. The procedure finishes when fracture happens. Data gathered (F, l, A_0, l_0) can be employed to define different quantities using Formulas (1.1),(1.2),(1.3),(1.4); [1],[2],[3].

$$\sigma_{eng} = \frac{F}{A_0} \tag{1.1}$$

$$\varepsilon_{eng} = \frac{l - l_0}{l_0} \tag{1.2}$$

where

- F: the tensile force applied;
- A_0: initial cross section area;
- A: actual cross section area;
- l: actual length;
- l_0 actual length;

Whereas the true stress σ_{true} and true strain ε_{true} are [3]

$$\sigma_{true} = \frac{F}{A} \tag{1.3}$$

$$\varepsilon_{true} = \ln\frac{A_0}{A} = \ln\frac{l}{l_0} \tag{1.4}$$

Quantities coming from Formulas (1.1),(1.2), are required to plot the well known engineering stress-strain curve, whereas Formulas (1.3),(1.4) are required to get the true stress-strain curve.

Equations (1.3),(1.4) can represent, for a random material, the graph plotted in Figure 1.2b; to describe such behavior, several models have been developed, but one of the most suitable for metals is the so called Ramberg-Osgood model [2]

$$\varepsilon = \varepsilon_{el} + \varepsilon_{pl} = \frac{\sigma}{E} + \left(\frac{\sigma}{K}\right)^{\frac{1}{m}} \tag{1.5}$$

where

- E: elastic modulus or Young's modulus;
- K: cyclic strength coefficient;
- m: cyclic hardening exponent;
- ε_{el}: elastic strain;
- ε_{pl}: plastic strain;

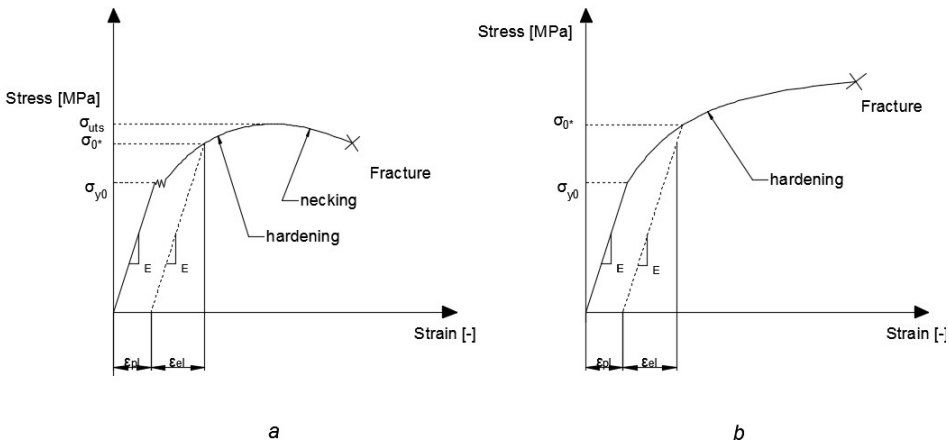

Figure 1.2: Engineering stress-strain curve Figure a,True stress-strain curve Figure b.

In Figure 1.2 others meaningful parameters are shown:

- σ_{uts}: Ultimate tension strength;
- σ_{y0}: Yield stress (stress evaluated when a permanent strain of 0.02 % is reached);
- σ_{0*}: Actual yield stress;

1.1.2 Effect of cyclic loading

The load applied to a specimen for traction testing, can be defined imposing a certain stress or strain . If it is considered a material subject to alternative strains $\pm\varepsilon$, the true stress-strain curve of the first cycle can be plotted in the Figure 1.3.

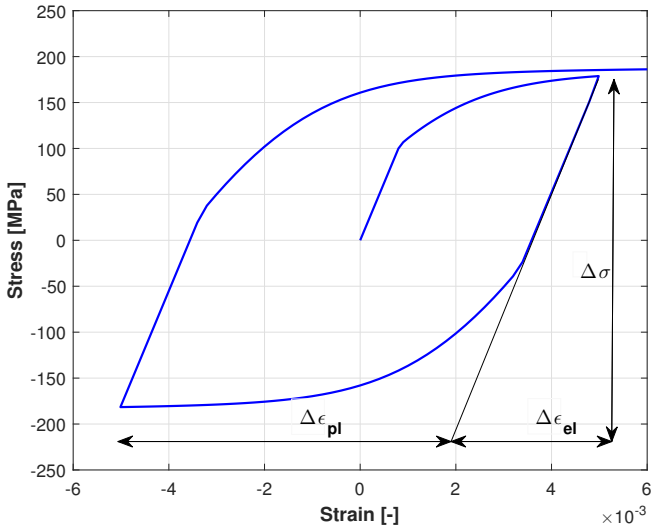

Figure 1.3: Stress-strain loop.

The total strain range can be decomposed in elastic strain range (difference between maximum and minimum elastic strain) and plastic strain range (difference between maximum and minimum plastic strain) [1],[2],[3].

$$\Delta\varepsilon = \Delta\varepsilon_{el} + \Delta\varepsilon_{pl} \tag{1.6}$$

Taking into account $\Delta\varepsilon_{el}$, it corresponds clearly to the ratio between stress range ($\Delta\sigma$) and elastic modulus[1],[3]:

$$\Delta\varepsilon_{el} = \frac{\Delta\sigma}{E} \tag{1.7}$$

Further, defining the stress amplitude $\sigma_a = \Delta\sigma/2$ the strain amplitude can be assesses as [2]:

$$\varepsilon_a = \frac{\sigma_a}{E} + \varepsilon_{pl,a} \tag{1.8}$$

Where $\varepsilon_{pl,a}$ is the plastic strain amplitude. Equations (1.7) and (1.8) are influenced by many factors such as environment temperature, kind of material,

etc.. These factors can influence, slightly or not the behavior under cyclic loading, for this reason different categories, that relate cyclic stress-strain relation, can be observed [1],[2],[3]. These are: hardening, softening and combination of hardening and softening.
When cyclic loading is applied some examples of hardening can be found in Figure 1.4. In the firs one applying a constant strain range, the material stress's increase; in the other case applying a constant stress range the strain decreases. On the other hand, when stress range decrease under imposition of an alternative strain, softening will occurs (Figure 1.5). A criteria, to distinguish between hardening and softening, takes into considerations data coming from uniaxial tensile test [10]. In Figures 1.4,1.5 [3] are shown the most typical behavior.

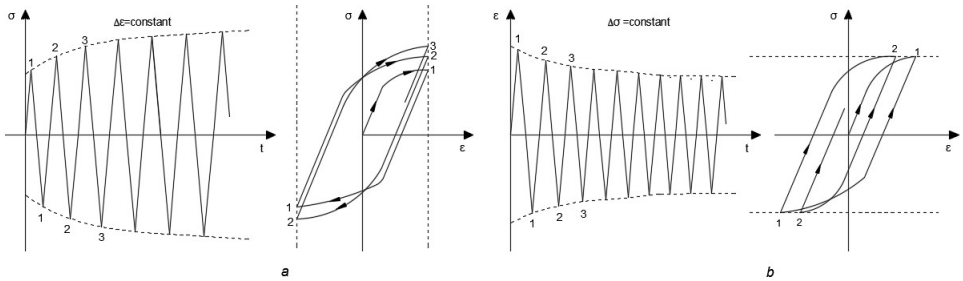

Figure 1.4: Phenomena of cyclic hardening. Material exhibits a growth of stress range applying a constant strain range (a); Material exhibits a reduction of strain applying a constant stress range (b).

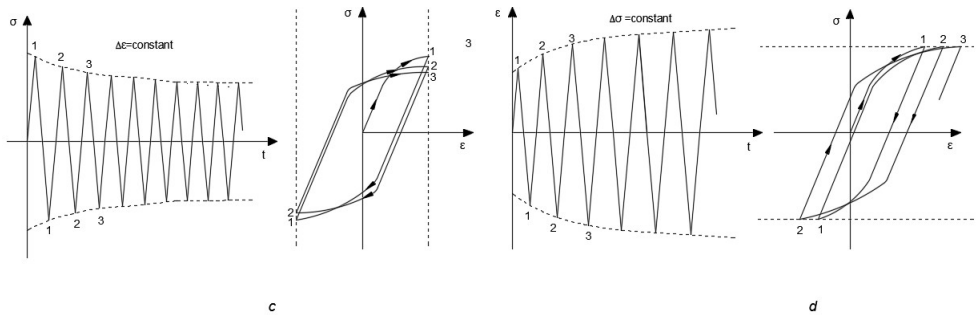

Figure 1.5: Phenomena of cyclic softening. Material exhibits a reduction of stress range applying a constant strain range (a); Material exhibits a growth of strain applying a constant stress range (b).

1.2 Tensor notation

Extension from mono-axial stress state case to tri-axial stress case can be done using tensors. Some useful formulas can be written and such will be exploited for managing plasticity theories [2].
Stress tensor $\underline{\sigma}$ and strain tensor $\underline{\varepsilon}$ are defined as follow [2].

$$\underline{\sigma} = \begin{bmatrix} \sigma_x & \tau_{xy} & \tau_{xz} \\ \tau_{yx} & \sigma_y & \tau_{yz} \\ \tau_{zx} & \tau_{zy} & \sigma_z \end{bmatrix} \quad ; \quad \underline{\varepsilon} = \begin{bmatrix} \varepsilon_x & \gamma_{xy} & \gamma_{xz} \\ \gamma_{yx} & \varepsilon_y & \gamma_{yz} \\ \gamma_{zx} & \gamma_{zy} & \varepsilon_z \end{bmatrix}$$

The unit tensor is [2]:

$$\underline{I} = \begin{bmatrix} 1 & 0 & 1 \\ 0 & 1 & 0 \\ 0 & 0 & 1 \end{bmatrix}$$

The stress tensor can be decomposed into a deviatoric ($\underline{A}$) stress tensor and a hydrostatic ($\underline{B}$) stress tensor[2]:

$$\underline{\sigma} = \underline{A} + \underline{B} \tag{1.9}$$

$$\underline{B} = \frac{1}{3}(\underline{\sigma} : \underline{I})\underline{I} \tag{1.10}$$

In standard engineering books, the definition of the inner product between tensor happens with the next formula :

$$\underline{\sigma} : \underline{\varepsilon} = \sum_{i=1}^{n} \sum_{j=1}^{n} \sigma_{ij} \varepsilon_{ij} \tag{1.11}$$

The total strain increment tensor ($d\underline{\varepsilon}$) is assumed and expressed as the sum of elastic strain increment tensor and plastic strain increment tensor [2][3]:

$$d\underline{\varepsilon} = d\underline{\varepsilon}_{el} + d\underline{\varepsilon}_{pl} \tag{1.12}$$

Assuming that Hooke's law is applicable, the elastic strain can be expressed by equation (1.13)[2]

$$d\underline{\varepsilon}_{el} = \frac{1+\nu}{E}\left[d\underline{\sigma} - \frac{\nu}{1+\nu}(d\underline{\sigma} : \underline{I})\underline{I}\right] \tag{1.13}$$

Where

- $d\underline{\sigma}$: stress increment tensor;
- G: Elastic shear modulus;
- ν: Poisson ratio;

1.2.1 Plasticity theories

The yield surface is a function that defines the bound between elastic and plastic domain, under any multiaxial state of stress[2].

$$f(\underline{A}) < 0 \tag{1.14}$$

(1.14) represents the criteria for defining elastic domain.
In literature there are several models which define the bound of elastic domain, but the most suitable for metals is Von Mises criteria[1][2].

$$f(\underline{A}) = \frac{3}{2}\underline{A} : \underline{A} - \sigma_{y0}^2 = 0 \tag{1.15}$$

Hence the Von Mises stress σ_{vm}, also called equivalent stress can be written as follow [1][2]:

$$\sigma_{vm} = \frac{1}{\sqrt{2}}\sqrt{(\sigma_{11}-\sigma_{22})^2(\sigma_{22}-\sigma_{33})^2(\sigma_{33}-\sigma_{11})^2} \tag{1.16}$$

Once the elastic limit is reached, a relation among stress increment and plastic strains increment is required. Hence the actual plasticity tensor is defined as [2]:

$$d\underline{\varepsilon}_{pl} = d\lambda \frac{\partial f(\underline{A})}{\partial \underline{\sigma}} \tag{1.17}$$

where $d\lambda$ is a positive scalar, which is non zero only when plastic deformation occurs [2].
When plastic domain is reached if the load decreases, trivially the elastic behavior occurs again whereas if the load increases the yield surface changes its dimension for this reason it is called loading surface. The loading surface can change size, shape, position. From this concept lots of problems bear, so the purpose of hardening theories is to determine how the loading surface changes its shape and its position from the initial reference frame after a single or multiples repetitions applying a certain load.

1.3 Hardening models

Basically the most important hardening models are kinematic models, isotropic models, and combined models, nevertheless other models will be presented and used more ahead. Hardening models have been developed in order to forecast material behavior when cyclic loading occurs, trying to achieve a correspondence with experimental data and verify if stabilized conditions will occur or not. A stabilized condition happens when the loading surface doesn't change anymore its position and its shape [1].

1.3.1 Kinematic models

Kinematic hardening model states that when plastic deformation occurs, the yield surface translates in the stress domain(Figure 1.6a) without changing its size, shape and orientation[2].
Considering the Von Mises criteria the yield function can be written as[2][3]:

$$f(\underline{A}, \underline{\alpha}) = \frac{3}{2}(\underline{A} - \underline{\alpha}) : (\underline{A} - \underline{\alpha}) - \sigma_{y0}^2 = 0 \tag{1.18}$$

$\underline{\alpha}$ represents the back stress tensor which defines the position of the loading surface. So far, in literature many efforts have been focused to understand how to describe the back stress tensor. Figure 1.6 represents respectively a linear kinematic model (b) and a nonlinear kinematic model (c)[2][3].

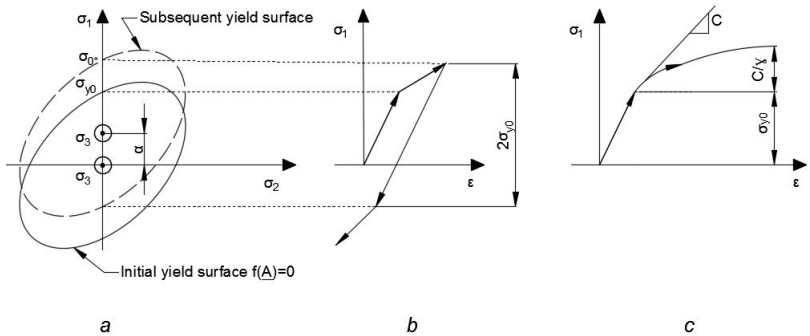

Figure 1.6: Kinematic models. Translation of the yield surface (a); Linear kinematic model(Prager model) (b); nonlinear kinematic model (Armstrong and Friederick model)(c).

From Figure 1.6c can be defined:

- γ: nonlinear recovery parameter or rate of stress saturation (it depends from temperature), it determines the rate of stress saturation;
- C: initial plastic modulus;

Linear kinematic model implies the presence of a linear relation among the variation of $\underline{\alpha}$ and the variation of the plastic strain [1], an example is given from equation (1.19).

$$d\underline{\alpha} = \frac{2}{3} C d\underline{\varepsilon}_{pl} \tag{1.19}$$

Nonlinear kinematic model states that the position's variation of the loading surface, changes nonlinearly with the variation of the accumulated plastic strain. This new term is defined as follow[1][2]

$$d\varepsilon_{pl,acc} = \sqrt{\frac{2}{3} d\underline{\varepsilon}_{pl} : d\underline{\varepsilon}_{pl}} \tag{1.20}$$

In this case the formula that links the stress back tensor and and the plastic strain increment tensor is [1] :

$$d\underline{\alpha} = \frac{2}{3} C d\underline{\varepsilon}_{pl} - \gamma \underline{\alpha} d\varepsilon_{pl,acc} \tag{1.21}$$

Moreover Figure 1.6c shows a saturation conditions is achieved by the actual yield stress, indeed it reaches a limit value equal to the sum of the initial yield stress and the ratio between the initial plastic modulus and the nonlinear recovery parameter (C/γ).

1.3.2 Isotropic model

Isotropic hardening model assumes that the initial yield surface enlarges uniformly without changing its center and orientation [1][2].
The yield function can be written through equation (1.22) [1][2]

$$f(\underline{A}) = \frac{3}{2} \underline{A} : \underline{A} - \sigma_{0*}^2 = 0 \tag{1.22}$$

with

$$\sigma_{0*}^2 = (\sigma_{y0} + R)^2 \tag{1.23}$$

- R : isotropic hardening function;
- σ_{y0}: initial yield stress;
- σ_{0*} : actual yield stress;

Isotropic models can be divided in linear isotropic models (Figure 1.7b) and nonlinear isotropic models (Figure 1.7c). Exploiting the nonlinear isotropic model the evolution of the isotropic hardening function may be expressed by equation (1.24) [1][2]

$$dR = b(R_\infty - R) d\varepsilon_{pl,acc} \tag{1.24}$$

in which are used:

- b: speed of stabilization;
- R_∞: saturation stress;

In Figure 1.7c the actual yield stress increases toward a limit value called saturation stress [2][3].

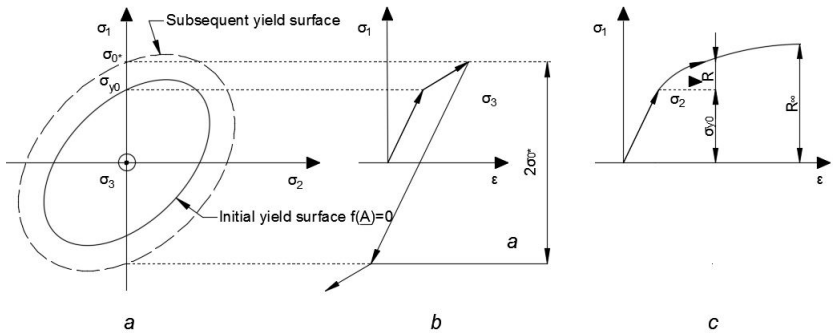

Figure 1.7: Isotropic models. Enlargement of the yield surface (a); linear isotropic model; nonlinear isotropic model (b).

1.3.3 Combined model

Combined model is obtained by combination of nonlinear isotropic model and nonlinear kinematic model [1], the yield criteria can be written with equation (1.25) [1][2].

$$f(\underline{A}) = \frac{3}{2}(\underline{A} - \underline{\alpha}) : (\underline{A} - \underline{\alpha}) - (R + \sigma_{y0})^2 = 0 \tag{1.25}$$

In this case a threshold value of the actual yield stress is presented with equation (1.26)[2][3]

$$\sigma_{max} = \sigma_{y0} + \frac{C}{\gamma} + R_{\infty} \tag{1.26}$$

In figure 1.8 it possible to see simultaneously the combination of enlargement and translation of the loading surface. Moreover in right side of the same figure is shown the amount of the actual yield stress when stabilization is reached.
A noticeable point regards the application of this model for metals; when cyclic loading is applied, this model allows to obtain reliable data close to experimental tests.

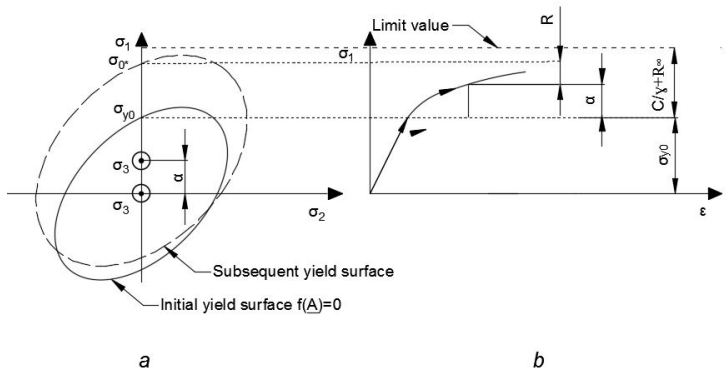

Figure 1.8: Combined model; the left side is focused on show the enlargement and the translation of the loading surface; in the right side is plotted the correspondent stress-strain curve.

1.4 Others models

In this work others models will be useful more ahead, they are:

- Accelerated models: these models exploit the combined model using speed of stabilization's values greater, in order to have a model which reaches that stabilized conditions quicker. [3],[1]
- Stabilized model: this model uses the same concepts of nonlinear kinematic model exploiting data (about yield stress and elastic modulus) coming from tensile test for a material which is in stabilized conditions.[3][4]

Chapter 2
Analysis of main plasticity parameters

2.1 Model analyzed

The purpose of this charpter are mainly two:

- Understand how material parameters defined in the previous chapter influence cyclic behavior of a component. This will be possible through computational simulations with a finite element software.
- Perform a comparison among two finite element softwares (Ansys and Marc Mentat) through the computational simulations required in the previous point.

It has been chosen that the component that will undergo the computational simulations has the characteristics shown in Figure 2.1.

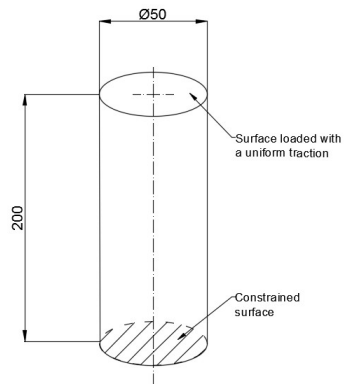

Figure 2.1: Component's geometry and loading conditions (dimensions: mm).

The geometry just depicted is a clear case of axially-symmetrical body. This features can be exploited in the finite element softwares to represent the corresponding geometry in two dimension, thereby saving elements, nodes and hence computational time.
Finally, to see plasticity it has been set a traction load through imposition of a displacement equal to 1 mm, that changes following the trend imposed in Figure 2.2.

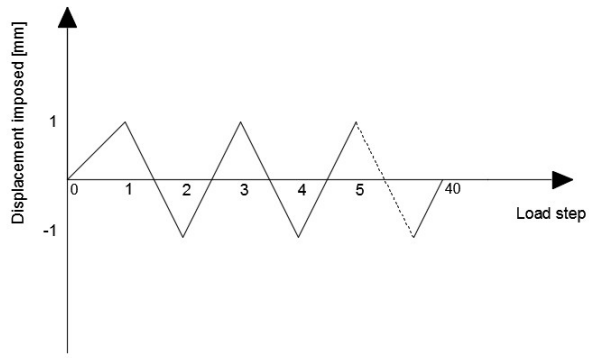

Figure 2.2: Loading history.

Once the geometry is defined the next steps are required to obtain the computational model: element's setting, material properties setting, application of a mesh, application of boundary conditions. In the end a sensitivity analysis (aimed to optimize the mesh) is performed to have a trade off between solution's reliability and computational time. For instance using Marc Mentat the result of these steps is in Figure 2.3.

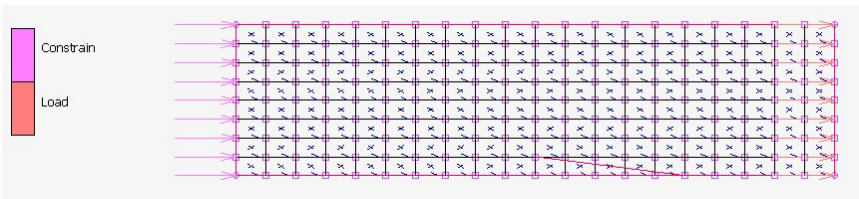

Figure 2.3: Model's geometry with boundary conditions and mesh, using Marc Mentat.

In Figure 2.3 the constrains and the loads applied are shown by mean of vectors. Obviously a displacement equal to zero is represented through the constrain whereas a displacement equal to 1mm represent the load. Furthermore the red line close to the middle part identify a surface. The position is

horizontal cause the software assume automatically the axial-symmetry from axis X.

At this point it has been listed in Table 2.1 the material properties required; they are available in book [3].

E (GPa)	σ_{yo} [MPa]	ν[–]	C [MPa]	γ [-]	R_∞ [MPa]	b [-]
125	100	0.36	64257	888	76	8

Table 2.1: Properties Cu-Ag alloy.

2.1.1 Finite element used for the simulations

Particular attention has been payed in a key phase, the choice of the finite element . For Ansys simulation the element 'Plane 183' is used; It is a 2D element composed by 8 nodes having 2 degrees of freedom through translations in nodal x and y directions, it has quadratic displacement behavior[8].
About Marc Mentat, in order to perform the simulations in the same conditions a similar finite element has been chosen in the available library. 'Element 28' in Marc presents some main characteristics. It is suited for axial-symmetric applications, It has 8 nodes having 2 degrees of freedom. Finally the both elements should have the same behavior.

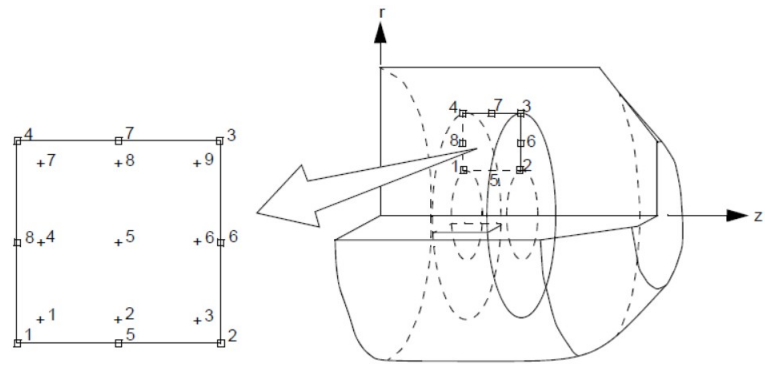

Figure 2.4: Definition of 'Element 28' from the Marc guide.

2.2 Steps followed with Marc Mentat

Here, a brief explanation of the steps followed with Marc is provided. Once the geometry has been defined the command 'convert' has been applied to substitute the geometry with a set of elements. The subsequent steps concern the material properties, the boundary conditions, the definition of a load-case and

finally the 'job' settings; obviously these parts regards only the pre-processing, but before to go further let's see their main characteristics. Let's see now the reason of a key command: 'table'; in the command bar it is possible to find "Tables & Coord. Syst." , here is possible to define several different tables distinguished by physical and geometrical parameters. Moreover, if the definition of a table is too complex, using the command 'read' is possible to import data from a file. Thereby the defined table can represent different functions that have to deal with the phenomena studied; in our case the tables are very useful to perform the relation between time and load applied.
Subsequently it has been defined the geometrical properties, through the definition of the axially-symmetric properties in the relative part of the command bar.
One of the most important settings is covered by the material properties; here it has defined the yielding stress, the Young modulus, the Poisson's coefficient and the coefficients for plastic behavior. Having a good representation of reality is important to set all these parameters all well as the most suited yielding and hardening models or material models. About this last concept, to carry out the simulation, it has been used, Von Mises formula as yield criteria and Chaboche method for non-liner behavior (in Marc Mentat Chaboche method identify the combined model).

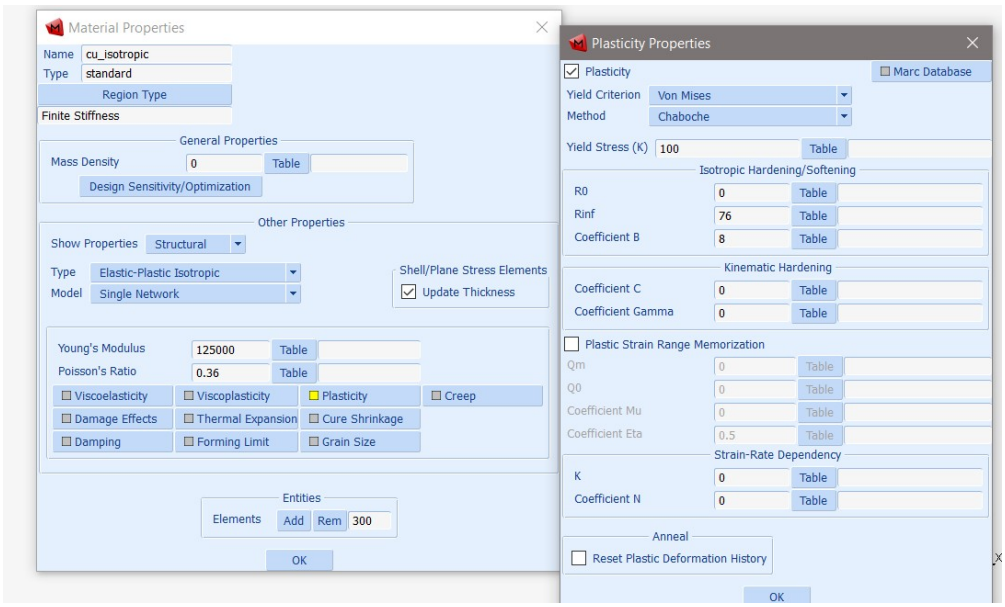

Figure 2.5: Material properties.

As we will see, to manage the simulation Ansys works differently from in Marc Mentat. Figure 2.5 supplies an example for the settings of the material properties and material model.

A notice is about Figure 2.5; several spaces are present with nearby the text 'table', it means that it is possible to fill the specific space with a table defined previously. After these settings the boundary conditions has been applied, imposing displacement zero on the nodes of the left side and displacement equal to one on the right side (Figure 2.3). Software Marc Mentat allows to declare multiple load-cases that means it is possible to combine in the same simulation different loading conditions.
The last step of the pre-processing is in section 'Job' in the command bar; here is possible to choose the load-cases that we want perform, and select the results that the software will show once the processing phase is ended. Details about this last phase are attached in Appendix.

2.3 Analysis of main kinematic and isotropic parameters with Marc Mentat

To do comparison it has been used a macro for Ansys that accomplish the task required in order to be always in the same conditions with Marc Mentat .
Several variables will be analyzed in applying the computational model defined. In order to avoid drawbacks, in the next simulations it is assumed that parameters missing the matching with a value, but required to perform the simulations, are taken from Table 2.1.
This section will presents how initial hardening modulus (C) and nonlinear recovery parameter (γ) influence plastic behavior when nonlinear kinematic model is applied. All this considering a transient in which the load gradually starts from zero to reach the imposed displacement.
All data will be gathered from the same region located in the center of the surface where the traction load is imposed.

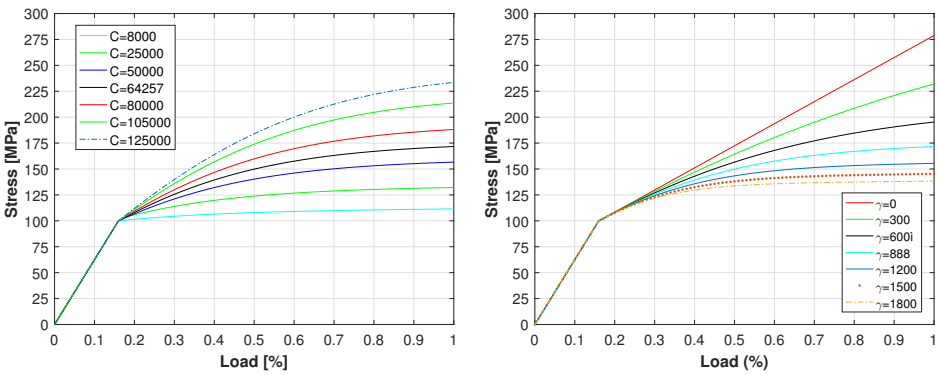

(a) Variation of C.

(b) Variation of γ.

Figure 2.6: Analysis of main kinematic parameters; variation of parameter C (a) and parameter γ (b) using Marc Mentat

Figure 2.6a shows that increasing the under investigated value the initial slope of the plastic region increases, moreover this fact determines that the actual yield stress increases as well. Figure 2.6b explains the meaning of γ; high values lead to achieve saturation conditions, contrariwise the low values lead to obtain a linear plastic region far from saturation condition.

In this second case it has been applied a nonlinear isotropic model to investigate what the speed of stabilization (b) and the saturation stress (R_∞),

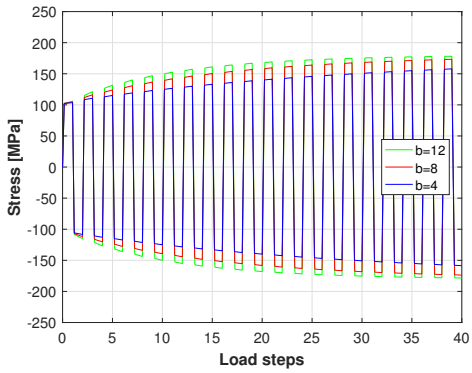

(a) Variation of the speed of stabilization b.

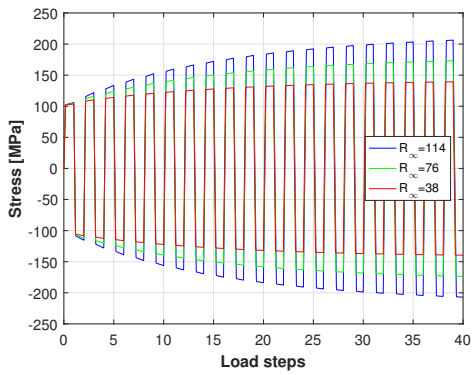

(b) Variation of R_∞.

Figure 2.7: Variation of parameter b (a) and parameter R_∞ (b) using Marc Mentat.

cause in such model. Now investigation is focused on cyclic behavior so Figure 2.7 will have in abscissa load steps correspondent with Figure 2.2.

With a certain number of load steps an increment of the speed of stabilization determines the reaching of higher values of actual yield stress, that means stabilized condition are achieved faster, an example of this behavior is supplied by Figure 2.7a.

How aforementioned in the previous chapter, R_∞ is the saturation stress and it determines the limit value of actual yield stress when isotropic model is applied. Applying the same speed of stabilization larger values of R_∞ will lead to higher value achieved by the actual yield stress. Figure 2.7b demonstrates this fact.

Finally exploiting the following data $R_\infty = 76\mathrm{MPa}$, $b = 8$ a simulation is carried out to plot the stress strain curve (Figure 2.8a) and its first and last cycle (Figure 2.8b)

Figure 2.8 shows morever that stabilization can be considered reached being the actual yield stress (of the last cycle) close to $\sigma_{y0} + R_\infty = 100 + 76 = 176[\mathrm{MPa}]$

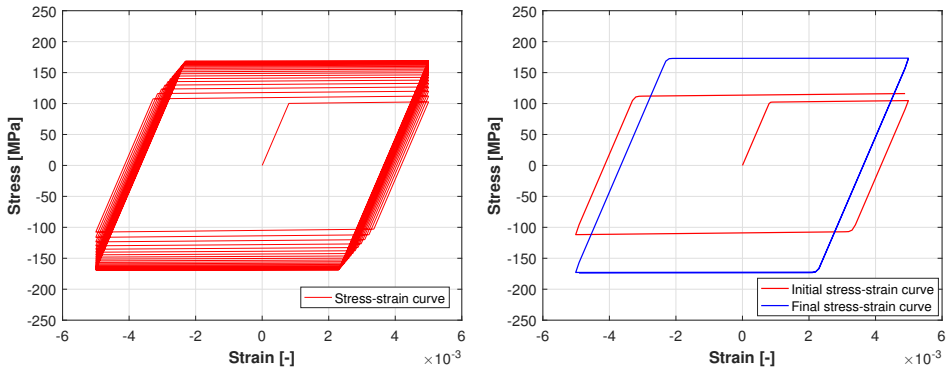

(a) Cyclic stress-strain curve. (b) Initial and final cycles.

Figure 2.8: Cyclic behavior with isotropic model using Marc Mentat.

2.4 Analysis of main kinematic and isotropic parameters with Ansys

To define the computationa model, the procedure followed with Ansys is quite similar,nevertheless some steps are different compared with Marc Mentat. First of all the material properties for linear behavior have been defined , hence for non-linear are chosen the options 'Von-Mises, isotropic, non linear' and just here are defined the relative parameters. Subsequently the geometry has been created , assigned the geometrical properties (axial-symmetric property) and defined the kind of finite element used (Plane 183).
Now, after the definition of the geometry and the the mesh (the same with Marc Mentat) we applied the property of axial-symmetric behavior along the Y-axis. Boundary conditions had been applied to simulate the loading already seen. Hence to permit a reliable comparison each simulation that will be carried out, will employ the material model. In the post-process, using the command 'History plot' all the data needed are obtainable to show the comparison.
Again the firsts simulations regards C and γ.

How it said before, C and γ are respectively the initial hardening modulus and the nonlinear recovery parameter or rate of stress saturation, hence the results obtained are the same with software Ansys. Every curve has the same trend and values of Figure 2.6.

Figures 2.10a,2.10b depict the variations of b,R_∞ , it is verified that using higher speed of stabilization the actual yield stress increase faster; moreover it is even verified again that a larger saturation stress leads to larger values achieved by the actual yield stress.

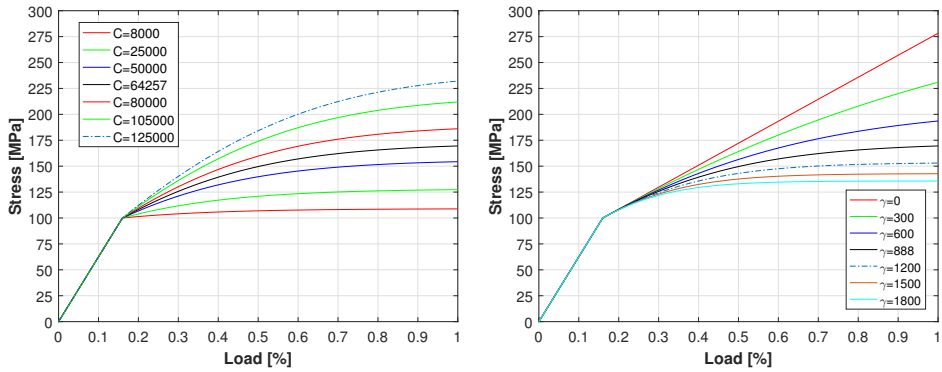

(a) Variation of C. (b) Variation of γ.

Figure 2.9: Variation of parameter C (a) and parameter γ (b) using Ansys.

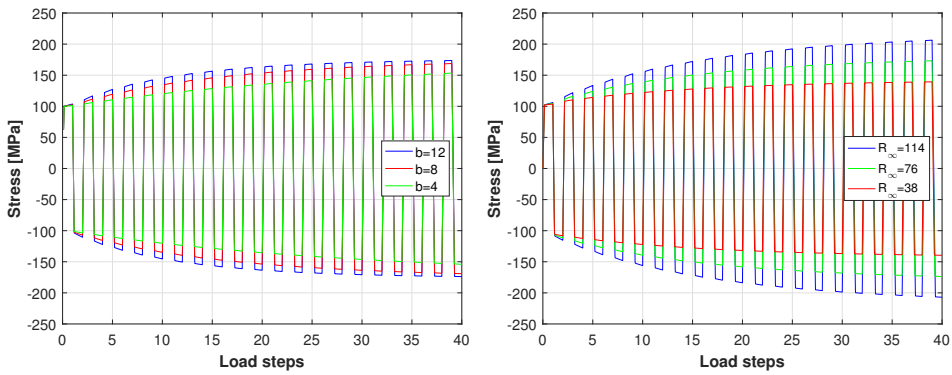

(a) Variation of b. (b) Variation of R_∞.

Figure 2.10: Variation of parameter b (a) and parameter R_∞ (b) using Ansys

Here in Figure 2.11 the stress strain curve is plotted wholly (Figure 2.11a) and its initial and final cycles (Figure 2.11b).

Again, results coming from Figure 2.11a allows to see stabilization being the actual yield stress (of the last cycle) close to $\sigma_{y0} + R_\infty = 100 + 76 = 176[MPa]$

Finished this phase a comparison of the most meaningful results can be done.

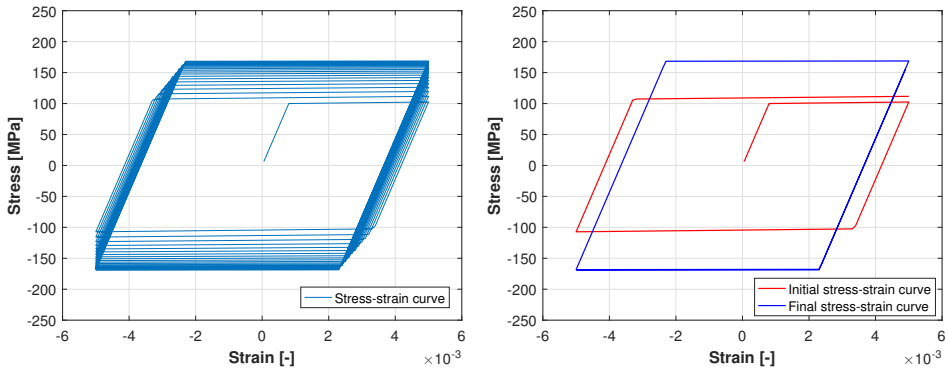

(a) Cyclic stress-strain curve. (b) Initial and final cycles.

Figure 2.11: Cyclic behavior with isotropic model using Ansys

2.5 Result's comparison

The first comparison concerns the difference between the initial and final cycles when an isotropic model is applied (the set of data comes from the previous simulations hence from Figure 2.8b and Figure 2.11b).

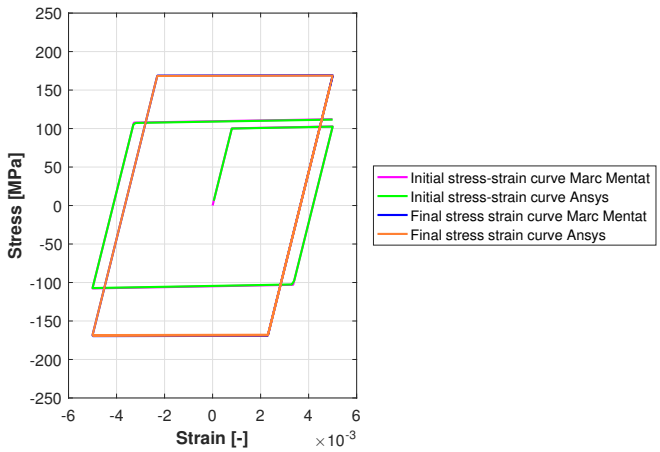

Figure 2.12: Comparison of obtained results regarding the first and the last cycle through a stress strain reference frame and the application of a nonlinear isotropic model

Figure 2.12 shows a very slight difference between the curve plotted. It corresponds to 2.23MPa and 2.26MPa for initial cycle and final cycle respectively. These are values under 2%.

The second comparison needs the follow hypothesis: it has been imposed an isotropic model with data coming from Table 2.1. It aims to see if the softwares behave in the same manner whether the displacement imposed changes. Figures 2.13,2.14 accomplish this task. The first Figure depicts results when the strain imposed is equal to 0.5%; the curve are almost superimposed, applying a strain equal to 2% appears a greater difference between the two curves, however in both cases stabilization is reached. The difference evaluated is about 4% , nevertheless the curve obtained with Marc Mentat overcomes slightly the limit value of the saturation stress.

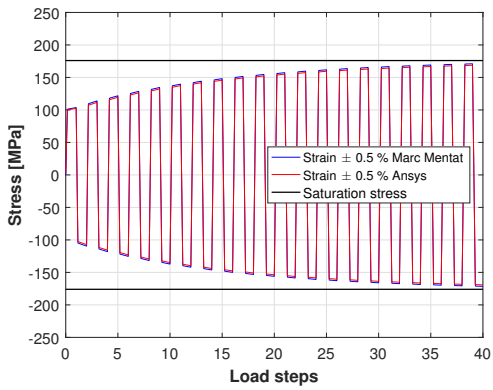

Figure 2.13: Dependence of strain applied.

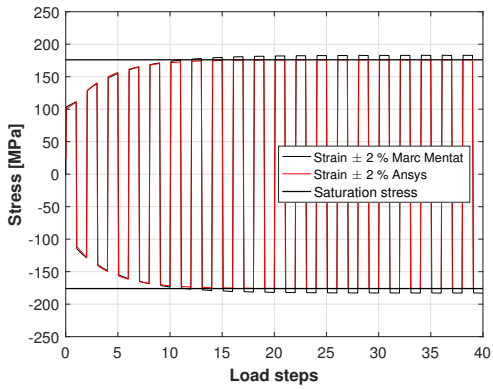

Figure 2.14: Dependence of strain applied.

Chapter 3
Case study: the casting mold

3.1 The casting mold

Continuous casting process is the most widespread technique to produce steel products such as bars, billets slabs etc. Such process is so widely used because it ensures important characteristics: high productivity, good quality, low costs; nevertheless the process is not without problems, indeed a continuous casting machine may produce slabs exhibiting surface defects such as cracks and deep oscillations marks. Among all the components of this system, one of the most critic is the casting mold. The mold is located close to the tundish, where the molten steel is cooled and first shaped [12] [13].

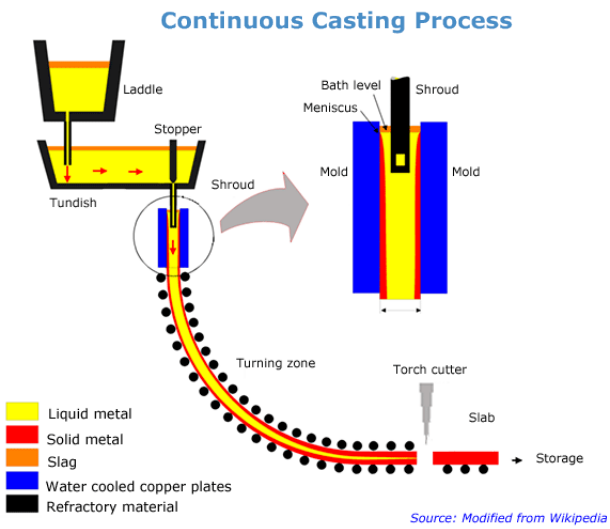

Figure 3.1: Continuous casting process of steel [6].

Therefore in this component the molten steel is thrown opportunely, in order to assume a certain shape and to start the solidification process. The working conditions imply that the molten steel is casted for several hours or days, until the system to cast is stopped (because of management reasons or for a failure). Again it is started and will then be stopped: such sequence determines the fact that the mold undergoes a cyclic thermal flux. Due to the high thermal flux exchanged, high temperatures, cyclic conditions and the aggressive chemical environment, the mold has a certain life and therefore it needs to be replaced with a new one after a certain number of castings [12] [13]. In Figure 3.1 the main components of a casting process are represented. The mold is usually made of a copper-silver alloy in order to transfer quickly the high thermal flux coming from the slag layer. The slag layer or rim layer is composed by powder put from the top to limit the thermal flux transmitted and to lubricate during the motion of the steel. When the steel comes out from the mold it continues to be cooled with spray injectors [12] [13].
This chapter will be focused on understanding how the mold is thermally and structurally stressed in cyclic conditions i.e. we will perform thermal-structural cyclic simulations using the software Marc Mentat.

3.1.1 Analyzed Geometry

The adopted geometry is brought from [14] and it is represented in Figure 3.2 and Table 3.1; the used unit of measure is mm.

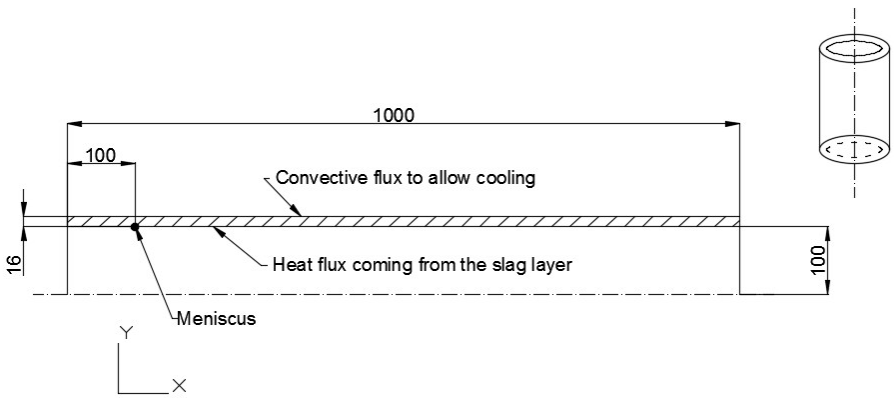

Figure 3.2: Geometry of the analyzed mold.

Main dimensions	Measure [mm]
Mold length	1000
Position of the meniscus from the top of the mold	100
Internal diameter	200
Outer diameter	232

Table 3.1: Main dimensions of the mold[14].

Figures 3.1 and 3.2 depict in the mold a region called meniscus; the meniscus is the region corresponding to the molten steel's level into the mold. Now, in order to define the numerical model, we provide a list about which parameters are taken into account and which factors are neglected:

- An axial-symmetry model is assumed;
- Large strain hypothesis are considered;
- A combined model is employed;
- A copper-silver alloy is being assumed [3];
- Thermal parameters (Thermal expansion, specific heat,thermal conductivity) are set using copper data available in standard material books.
- Boundary conditions are kept from [14];

On the other hand the following factors will be neglected:

- Static pressure of molten steel toward the internal surface is neglected due to its low value.

3.1.2 Material Properties

Basically copper is chosen to ensure a great heat exchange; this work has to deal with a copper-silver alloy whose mechanical properties are obtained from several test with different temperatures. These data are available in [3]. Homogeneous and isotropic properties are assumed. Experimental tests show that a combined model represents the best solution [3]. In the Table 3.2 there are all the structural data required for the computational analysis.
The Poisson coefficient is considered constant with temperature. All the data depending from temperature are computed by the software with linear interpolation. In Table 3.2 values of R_∞ are negative, that means a softening of the material will occur.

We can notice that R_∞ has at every temperature negative values, so it means that softening will occur.

Temp. [°C]	E[GPa]	σ_{y0}[MPa]	C [MPa]	γ[MPa]	R_∞[MPa]	b
20	119	130	42 250	617	−75.7	2.35
250	104	111	45 340	820	−80.2	3.89
300	103	110	40 080	832	−76.7	5.29

Table 3.2: Elastic modulus and yield stress data.

Now, once the geometry, the model's approximations, and the material's properties have been defined the next step regards the kind of element to use, the definition of the mesh, the boundary conditions.

3.1.3 Finite element used

The element used for this analysis is represented from 'element 28' [16]. Section 2.3 has already described this eight node arbitrary quadrilateral written for axial-symmetry element. Thermal properties are considered by the fact that element 28 during a coupled structural/thermal analysis is associated with element 42. This kind of element is written for axisymmetric heat transfer applications [16].

3.1.4 Mesh

To define a suitable mesh particular attention is required, mostly to avoid sources of error and for optimizing reliability of the solution and computational time. In order to achieve this goal the mesh is finer where an high gradient of thermal flux occurs, whereas it is rough in the region with almost constant thermal flux. Among these zones a different mesh is set to avoid large discontinuity between elements. Moreover, special care is put to maintain as much as possible the quadratic element thus keeping away from elements too enlarged in one dimension. After some attempts aimed to do a sensitivity analysis the mesh in Figure 3.3 is applied.

3.1.5 Loading conditions

Loading conditions covers a key role for the computed solutions; in this case they can be divided in structural and thermal boundary conditions.
In a continuous casting system the mold is kept in its position by means of hooks, so from a computational point of view the mold can be treated as a free body. Therefore one node is chosen to fix displacement along the length of the mold. Such node is chosen trivially to minimize its influence; Figure 3.4 shows, through the magenta arrow, the imposed displacement equal to zero in the farthest zone from the meniscus.
By the way of thermal boundary conditions, the uneven heat flux is set in the

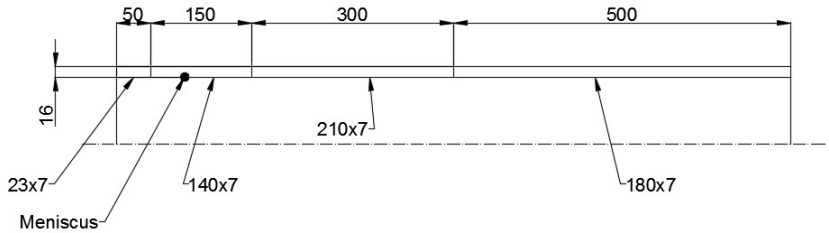

Figure 3.3: The mesh is shown through the product of the number of divisions along the length and the number of divisions along the thickness.

internal surface throughout the length of the mold; nevertheless it will be zero in the region forgoing the meniscus [14].
Cooling conditions are set throughout the outer surface imposing a convective flux determined by water at 40°C, [14] with a convective coefficient equal to 48000 $[w/(m^2K)]$ [14]. In the numerical model cyclic behavior will be determined by loading and unloading conditions; in loading conditions the heating and the cooling are properly imposed, whereas in the unloading phase it is set with cooling only coming from the water.

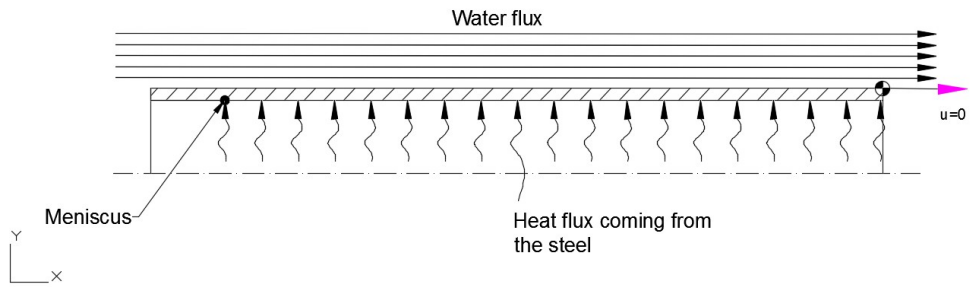

Figure 3.4: Applied boundary conditions.

Cyclical behavior can be schematically represented with Figure 3.5. The performed cyclic simulations will allow to obtain data in any computed time, nevertheless this work will use data coming from working or no working conditions when the thermal transient is ended i.e. when the mold will maintain the same temperature (obviously before another transient will occur).

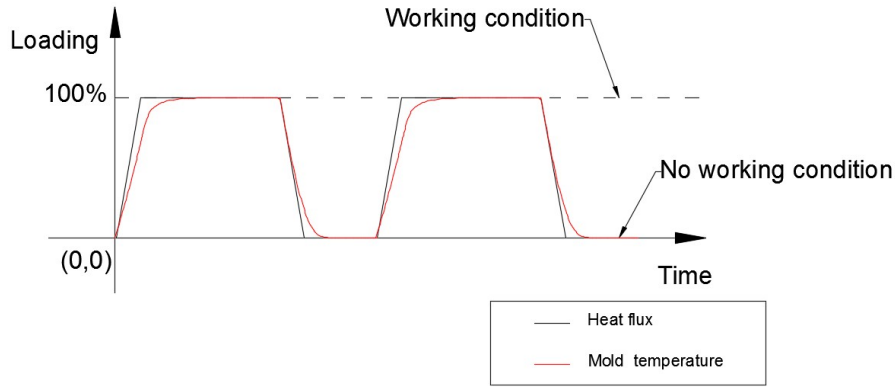

Figure 3.5: Representation of cyclic process.

3.2 Thermal analysis

With such working conditions, a thermal analysis has been computed to determine the temperature field of the mold once the thermal transient is finished. Figure 3.6 shows the obtained temperature field.

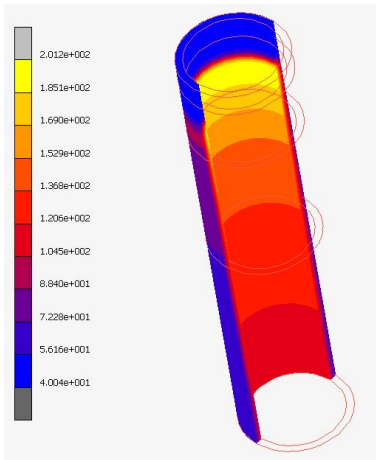

Figure 3.6: Temperature field (°C) in 3D.

Moreover Figure 3.7 is focused on localizing where the maximum temperature occurs and how much such temperature is far from the meniscus.

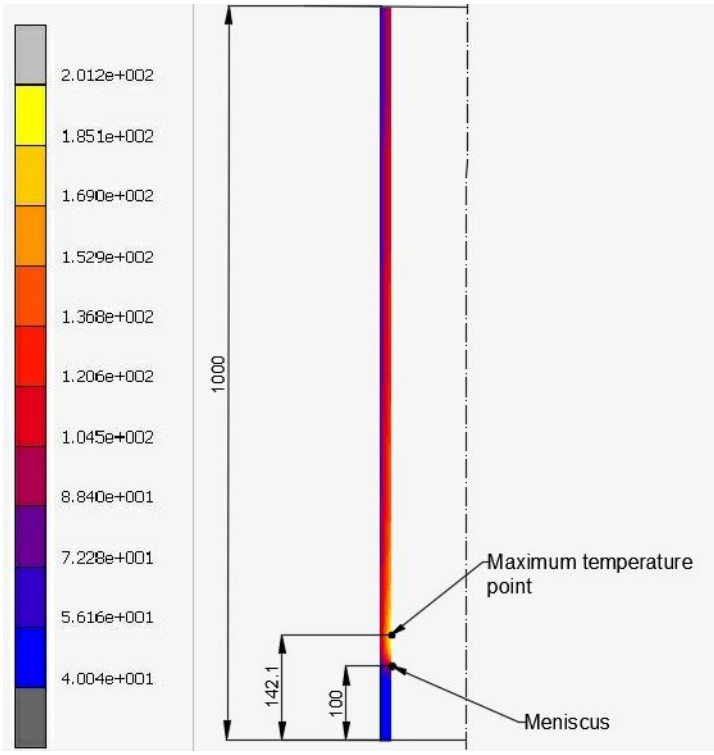

Figure 3.7: Temperature field in (°C) 2D.

Temperature profiles at the internal surface and outer surface are assessed by Figure 3.8

	Temp. [°C]	Loc. [mm]
$T_{max,in}$	201.2	142.1
$T_{max,out}$	90.6	147.5
$T_{min,in}$	40.1	0
$T_{max,out}$	40.1	0

Table 3.3: Temperature results.

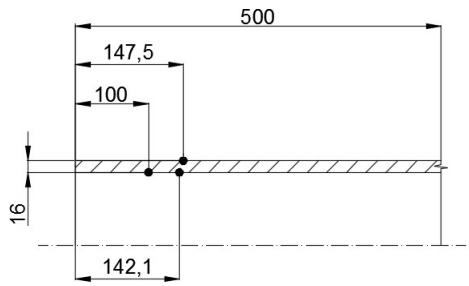

Figure 3.9: Temperatures location.

Ripples in the internal profile are tied with the ripples present in the thermal flux adopted [14]. Table 3.9 determines location of the minimum and max-

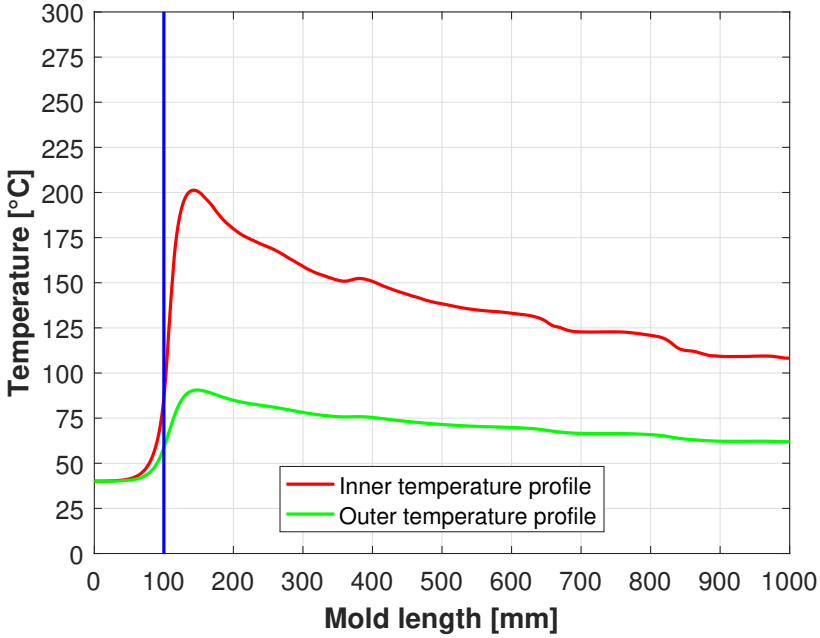

Figure 3.8: Temperature's profiles.

imum temperatures; the minimum temperatures occurs where the thermal flux is zero in the farthest zones from the meniscus.

3.3 Structural part

In this step a simulation will perform only one working condition, data are gathered when the thermal transient is ended. A thermal and structural coupled analysis is carried out: in this way axial, radial and circumferential stresses are depicted at internal and outer surface through Figures 3.10,3.11. The blue line identifies the position of the meniscus, hence it splits the region where molten steel flows from the thermally unloaded region. Subsequently maximum and minimum values are determined together with each location (Table 3.4 and Table 3.5). Finally the Von Mises stress profile is determined with Figure 3.12; the maximum values reached together with their position are in Table 3.6. The gathered data shows that achieved stresses overcome slightly the elasticity field in a small region around the meniscus.

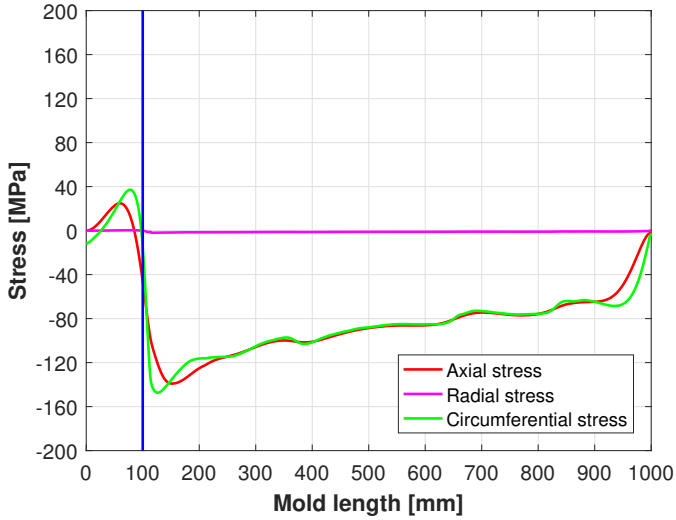

Figure 3.10: Stress distribution in the internal surface.

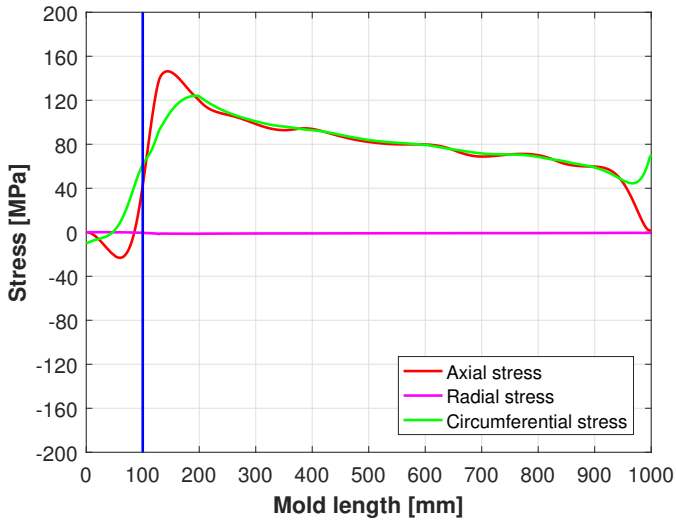

Figure 3.11: Stress distribution in the outer surface.

It is possible to notice from Figures 3.10,3.11, for internal surface and outer surface that in a large region the circumferential stress is close to the axial stress.
Obtained results have a physical meaning: in fact, in the internal surface the

Kind of stress	Max stress [MPa]	Location [mm]	Min stress [MPa]	Location [mm]
Axial stress	24.8	59	−139.1	149
Radial stress	0.3	0	−2.0	128
Circ. stress	37.2	78	−147.4	127

Table 3.4: Main stress values in the internal surface.

Kind of stress	Max stress [MPa]	Location [mm]	Min stress [MPa]	Location [mm]
Axial stress	146.3	144	−23.2	59
Radial stress	0.1	4	−1.6	128
Circ. stress	124.2	195	−10.1	0

Table 3.5: Main stress values in the outer surface.

	Max Von Mises stress [MPa]	Location [mm]
Internal surface	137.4	140
Outer surface	132.7	152

Table 3.6: Maximum values of Von Mises stress.

hottest region tries to expand much more than near zones, so a compression state arises.
Tables 3.4,3.5 supply values of the axial, radial and circumferential stress inside and outside the mold, with their locations.
Inside the mold, one can notice that Von Mises stress slightly exceeds the yielded stress in a small region around meniscus; moreover the maximum value occurs 4.7mm far from the maximum temperature position.
About this last concepts, several correspondences are noticed with references [12],[13][3].

3.4 Cyclic analysis

A working cycle is defined as the succession of a working condition and a no working condition. In this session the simulation will be performed on the mold for twenty cycles. In order to investigate the behavior of the most critic region [12] [13], the stress-strain curve of the element where the maximum temperature occurs will be plotted[12] [13].

So stress-strain curve are determined for axial(Figure 3.13a), radial (Figure 3.13b), and circumferential direction (3.14).

From these figures it is clear that softening does not occur due to the following reason. In the mold thermal flux determines an high and low stress

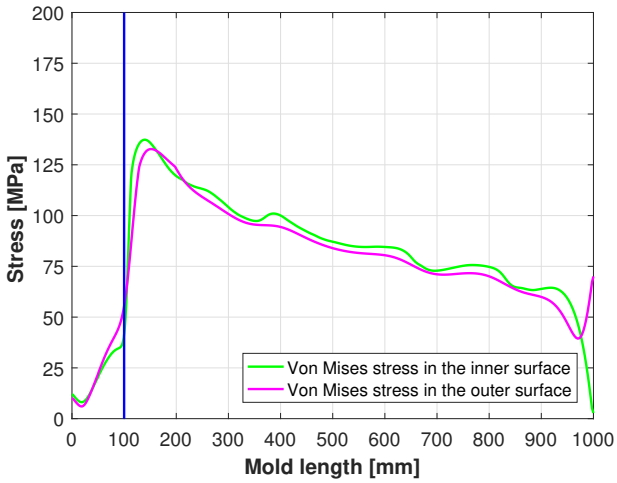

Figure 3.12: Distribution of Von Mises stress.

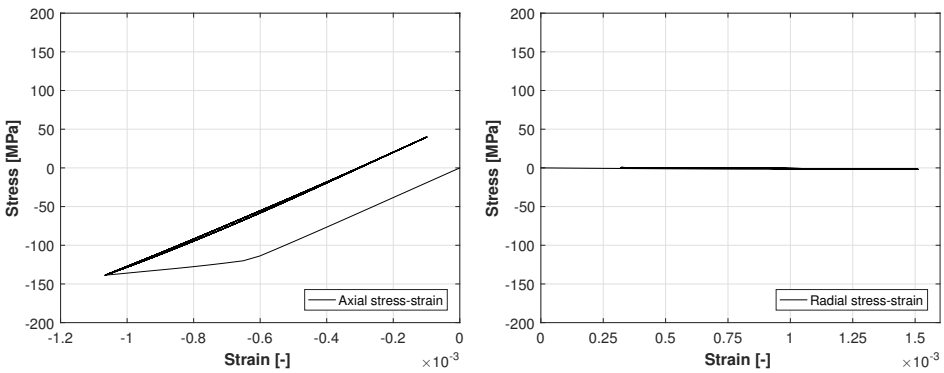

(a) Axial stress-strain curve.

(b) Radial stress-strain curve.

Figure 3.13: Axial stress-strain curve and radial stress-strain curve.

region; as it is demonstrated in the previous section the maximum stresses have reached values slightly over the yield stress; such values determine a certain actual yield stress that can't be overcome (because of the low value assumed) by the maximum stress in the next cycles. Hence, each of the stress-strain curves will superimpose itself in the next cycles remaining in the elastic domain. The responsible of this behavior is the stress achieved after half cycle, that is strictly determined by the combination of heating flux and cooling

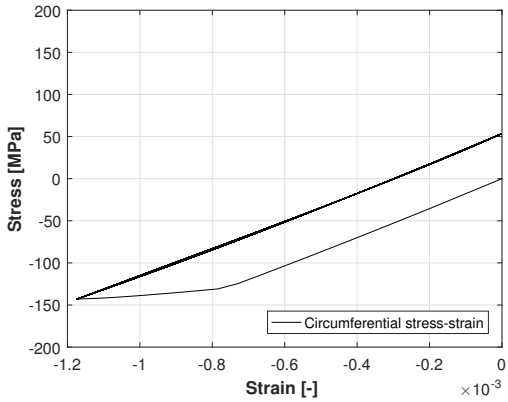

Figure 3.14: Circumferential stress-strain curve.

conditions imposed.
Finally, in order to perform a comparison of different plasticity models under cyclic conditions, it has been chosen to increase the thermal flux by 60%.

Temperature distribution profiles (Figures 3.8) and stress distribution profiles after a working condition (Figure 3.17) are determined again. The new max temperature is 297 °C, the remaining results are in the Tables 3.7, 3.8, 3.9.

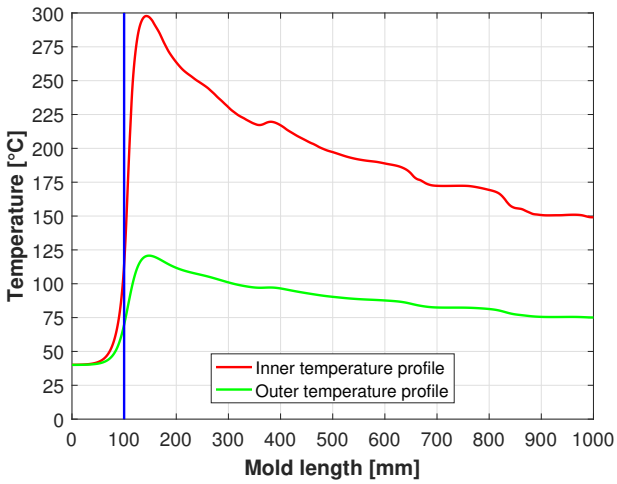

Figure 3.15: Temperature's profiles.

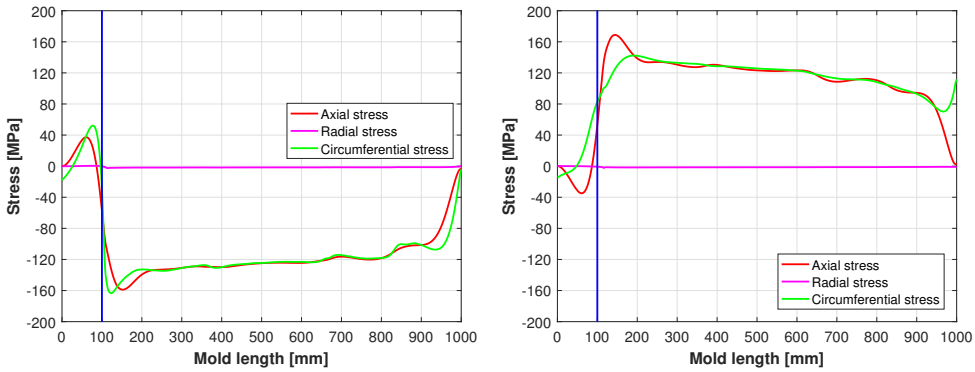

(a) (b)

Figure 3.16: Simulation obtained applying the new thermal flux; axial, radial and circumferential stress distribution in the internal surface (a); simulation obtained applying the new thermal flux; axial, radial and circumferential stress distribution in the the outer surface (b).

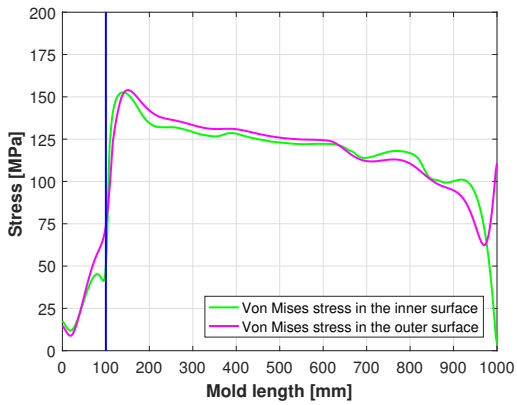

Figure 3.17: Von Mises stress with the new thermal flux.

.

Kind of stress	Max stress [MPa]	Location [mm]	Min stress [MPa]	Location [mm]
Axial stress	37.3	61	−158.8	152
Radial stress	0.5	1000	−2.5	115
Circ. stress	52.1	77	−163.3	124

Table 3.7: Main stress values in the internal surface.

Kind of stress	Max stress [MPa]	Location [mm]	Min stress [MPa]	Location [mm]
Axial stress	168.8	144	−34.8	61
Radial stress	0.1	4	−2.2	116
Circ. stress	142.3	191	−14.5	0

Table 3.8: Main stress values in the outer surface.

	Max Von Mises stress [MPa]	Location [mm]
Internal surface	152.6	140
Outer surface	154.0	151

Table 3.9: Maximum values of Von Mises stress.

Now, the goal is to understand when stabilized conditions are achieved by the models. This can be done by an approximate way, by means of equation (3.1) which represents a relation proposed in [1]:

$$2\mathfrak{b}\mathsf{N}\Delta\varepsilon_{\mathtt{pl}} \approx 5 \tag{3.1}$$

- N: number of cycles
- $\Delta\varepsilon_{\mathtt{pl}}$: Plastic strain range

This formula suggests that for this material, stabilized conditions will occur when the product between the speed of stabilization and the double of the accumulated plastic strain, approximately reaches the value 5. Thereby the number of cycles can be evaluated to perform the simulation; nevertheless this study has to deal with a multi-axial stress state. In this case after the evaluation of the three numbers of cycles, the lowest is chosen because (3.1) represents an upper bound where surely stabilization is reached. Such number of cycles is equal to 940. Finally, in every case where the number of cycles can be evaluated, the value of the plastic strain range is assessed after 10 cycles. Actually, sometimes the number of cycles is very large due to a small $\Delta\varepsilon_{\mathtt{pl}}$,so since results are required, a strategy can be used regarding the speed of stabilization setting. Following this concept, increasing parameter $\mathfrak{b}$ leads to acceleration of cyclic behavior but sometimes (due to too large values) it leads to

non-negligible error in the solution. This strategy will be applied and through a Matlab script (obtaining Figure 3.18), useful graphs to see stabilization will be shown.
The summary of the plasticity's model under investigations and the correspondent number of cycles expected is presented in Table 3.10

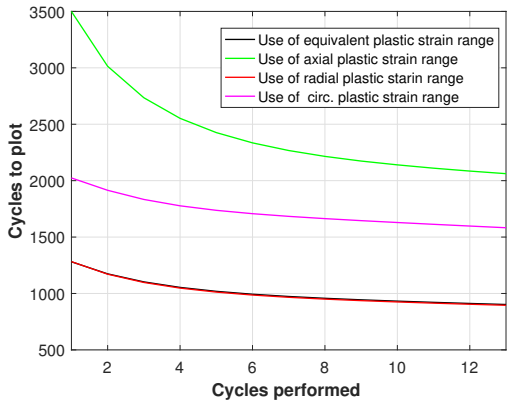

Figure 3.18: Example of graph obtained for the combined model.

Material model	Number of cycles expected
Combined	933
Acc. with $b = 10 * b_i$	44
Acc. with $b = 20 * b_i$	15
Acc. with $b = 40 * b_i$	7

Table 3.10: Number of cycles expected to reach stabilized conditions.

In the next sections we will perform simulations using different hardening models; the simulations have the goal to reach the stabilized conditions, and a common criteria is established 'a priori' for each case: stabilized conditions will be considered reached when the plastic strain range has a variation under 0.35% in the subsequent 10 cycles. So three values corresponding to each direction will be obtained, and the greatest will be taken as reference value.

3.5 Cyclic behavior using combined model

This first simulation uses the combined model. The next graphs show the stress-strain curve in axial, radial, circumferential direction applying 750 cycles. Figure 3.19d gives a representation of the stain range trend in any considered direction.

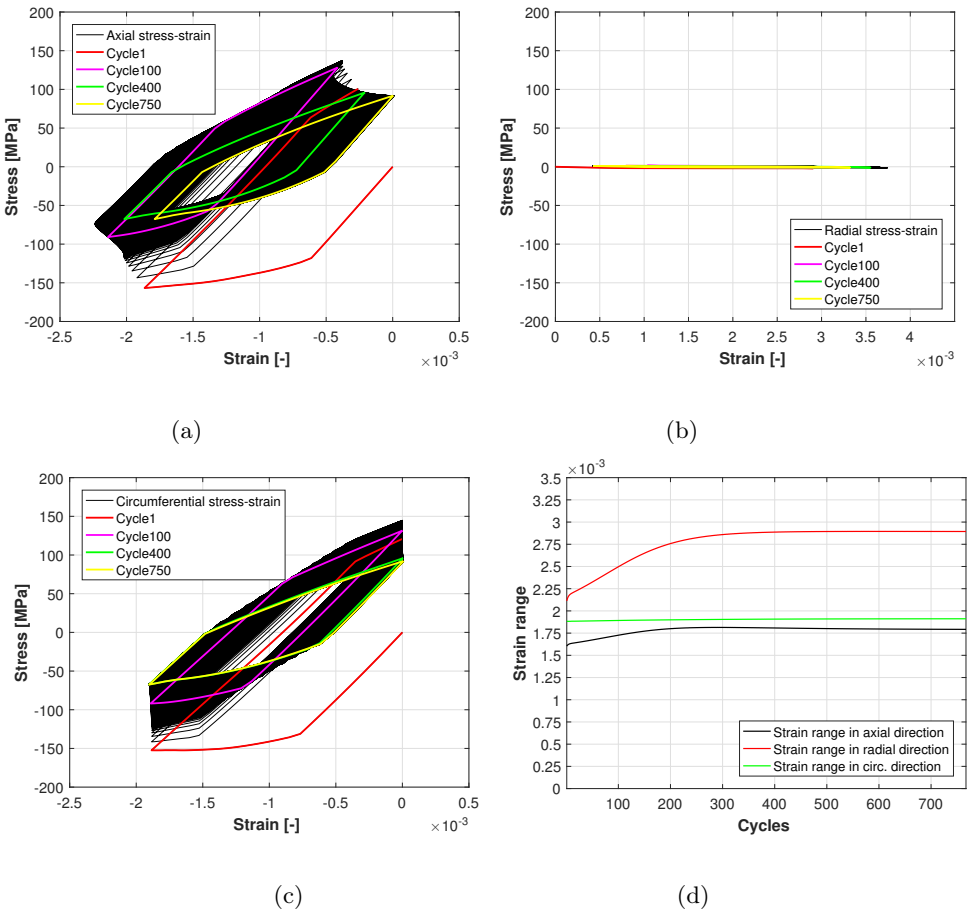

Figure 3.19: stress-strain curves for axial (a)radial (b) and circumferential direction (c), strain range curve (d).

The set of Figures 3.19 gives an idea about how material behaves, the plotted strain is obtained from sum of elastic and plastic strain. At first sight axial and circumferential stress-strain are quite similar because they have comparable values of stress whereas radial is very low (this is compliant with the lack

of internal and external pressure). This phenomenon means that a plane stress state happens in the considered region.
Focusing on Figures 3.19 it seems that stabilization is not reached, and Figure 3.19c instead shows the opposite because between cycle 400 and cycle 700 only a slight difference appears. In orderer to better understand, Figures 3.20a and 3.20b show plastic strain and stress trend.

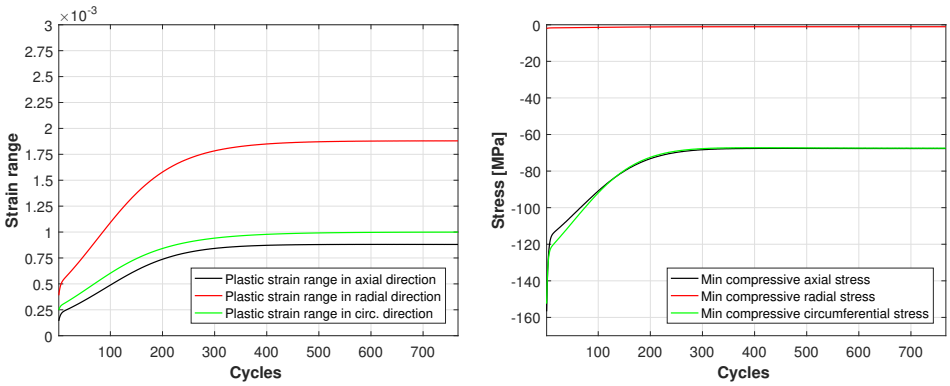

(a) (b)

Figure 3.20: Plastic strain range trend (a). Minimum compressive stress trend (b).

The graphs depicted in Figures 3.20a and 3.20b show clearly that stabilization can be considered as reached since the shape in the final part can be considered perfectly flat; moreover by applying the criteria defined in the previous section to Figure 3.20a, after 349 cycles stabilization is reached.

3.5.1 Accelerated model $\mathtt{b} = 10\mathtt{b}_\mathtt{i}$

The accelerated model has the purpose to reach faster stabilized conditions. This is possible maintaining a combined model, through variation of isotropic parameter $\mathtt{b}$. After performing 44 cycles it has been seen that the established stabilization criteria is not complied, so we chose an intermediate number of cycles to plot between the minimum and the maximum. For this reason we plotted 60 cycles.

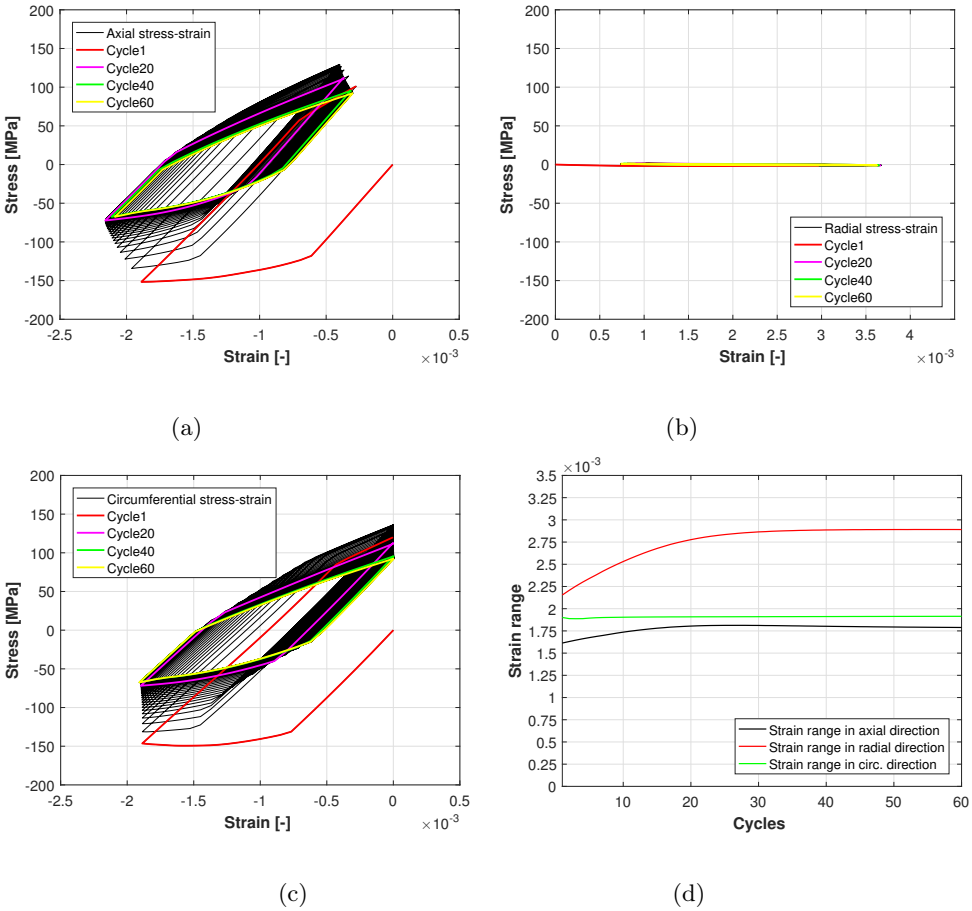

Figure 3.21: stress-strain curves for axial (a)radial (b) and circumferential direction (c), strain range curve (d).

From this set of figures, at first sight the same behavior and the values reached appears by comparing the sets of Figures 3.19,3.20. It will be shown

more ahead that this model allows a reduction of the computational time (since less cycles are being computed), maintaining almost the same solution obtained with the combined model.

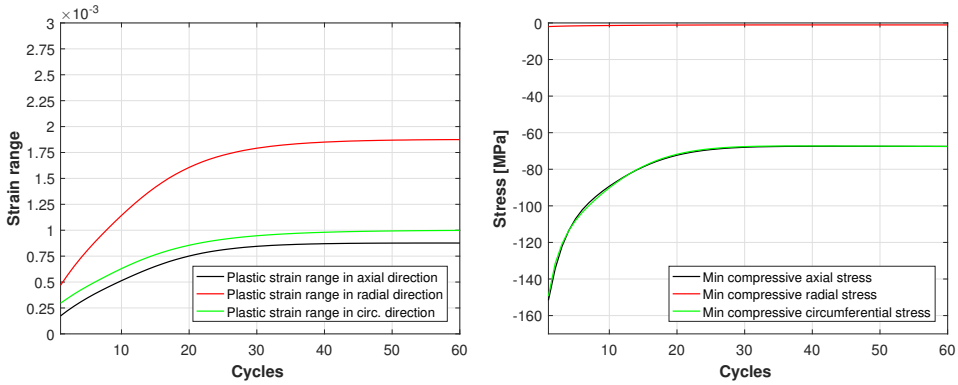

(a) (b)

Figure 3.22: Plastic strain range trend (a). Minimum compressive stress trend (b).

From the sets of picture contained in Figure 3.21,3.22 a slight different behavior starts to appear, regarding mostly strain range. However this difference is very small and can be considered negligible. In Figure 3.22b a perfect superposition happens in the whole cycle range, and since the initial values are greater comparing with 3.20, an estimation of the values of the stress is done. Nevertheless this is not enough to state in a wider sense that the model overestimates or underestimates.
Using the same criteria used in the previous case, stabilized conditions appears from cycle 58 (obviously such number is obtained after some attempts with more than 68 cycle).

3.5.2 Accelerated model $\mathtt{b} = 20\mathtt{b}_\mathtt{i}$

The same procedure is applied using $\mathtt{b} = 20\mathtt{b}_\mathtt{i}$, and the same procedure is adopted, nevertheless the same problem of subsection 3.5.1 regard the stabilized conditions appears again. To overcome this drawback the same steps are repeated; hence 30 cycles have been plotted.

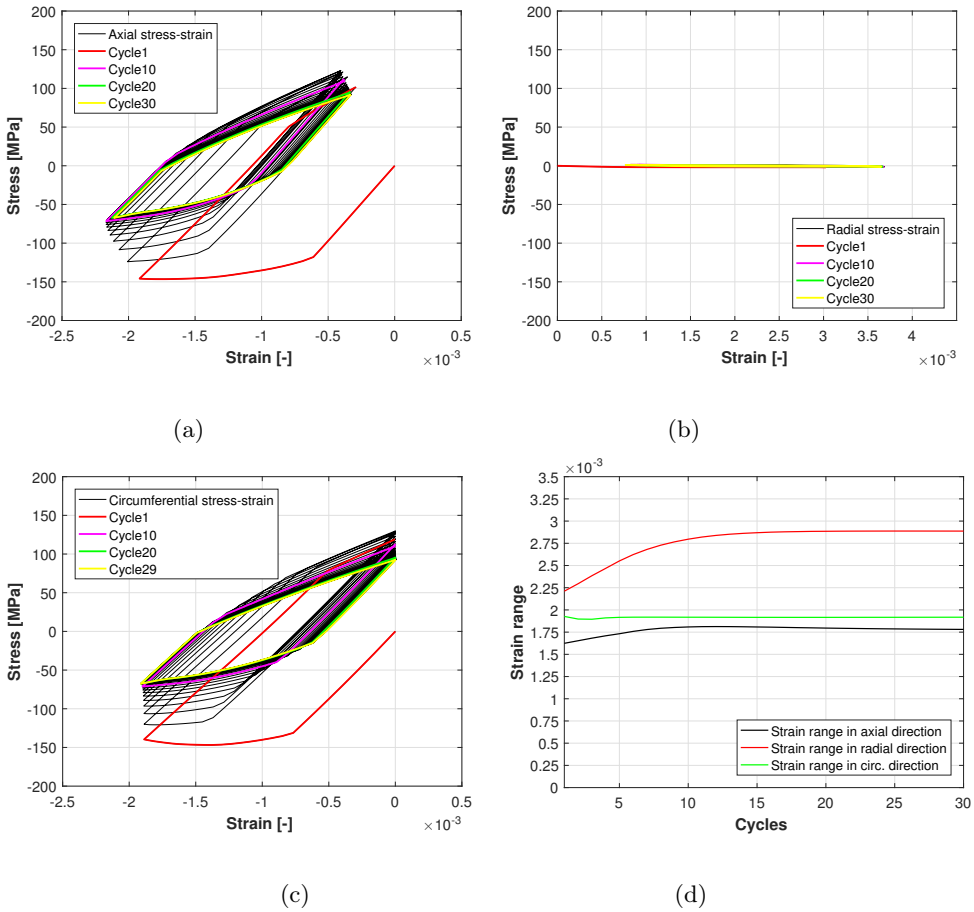

Figure 3.23: stress-strain curves for axial (a)radial (b) and circumferential direction (c), strain range curve (d)

Comparing 3.23 with 3.19 and 3.21 no particular difference is noticed about behavior or reached values. A deeper analysis of key values will be provided in the next section.

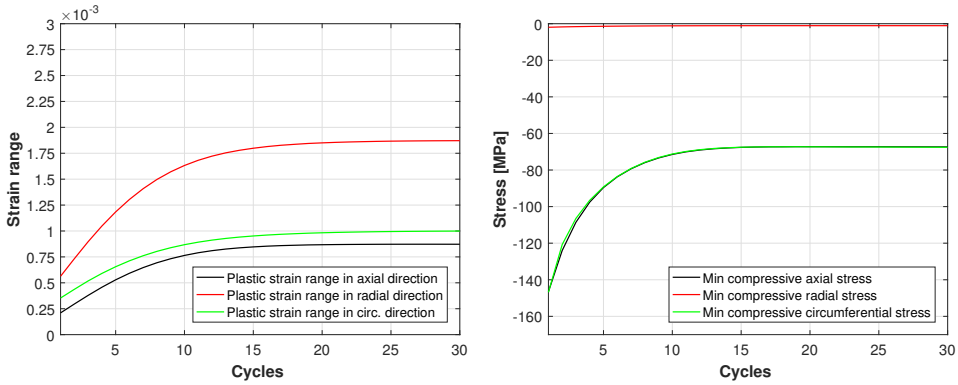

(a) (b)

Figure 3.24: Plastic strain range trend (a). Minimum compressive stress trend (b).

In this case applying the criteria defined in the previous chapter, the stabilized condition is reached after 28 cycles (as already stated in the previous subsection, such number is obtained after some attempts with more than 38 cycle).

3.5.3 Accelerated model $\mathtt{b} = 40\mathtt{b}_\mathtt{i}$

This attempt is done considering isotropic parameters $\mathtt{b} = 40\mathtt{b}_\mathtt{i}$, hence if the fist case uses a mean value of the speed of stabilization equal to 3.8 for the meximum temperature, in this one such values is 40 times higher, so about 154. Using again Formula 3.1 the evaluated values for $\mathtt{N}$ are $14, 12, 7$, but neither is enough to get stabilized conditions. Therefore, after some attempts it has been decided to plot 60 cycles. The results are presented in Figures 3.25 and 3.26

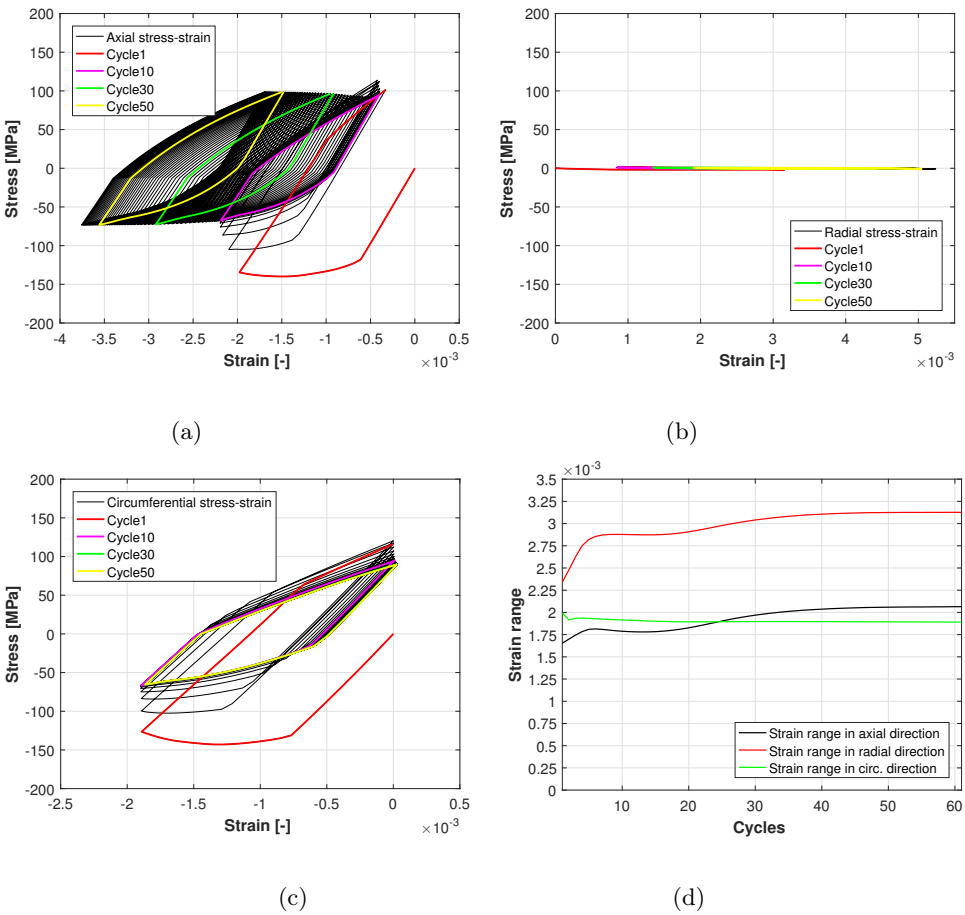

Figure 3.25: stress-strain curves for axial (a)radial (b) and circumferential direction (c), strain range curve (d).

It is clear that this model does not comply with the real physics. In every picture of set 3.25 reached values and assumed shape are too far from the first case in Figure 3.19. Important distortions are present in Figure 3.25a, 3.25b, 3.25c, and moreover 3.25d has oscillations. However the stabilization is reached and it states that after 51 cycles variation in the next 10 cycles is under 0.35% .

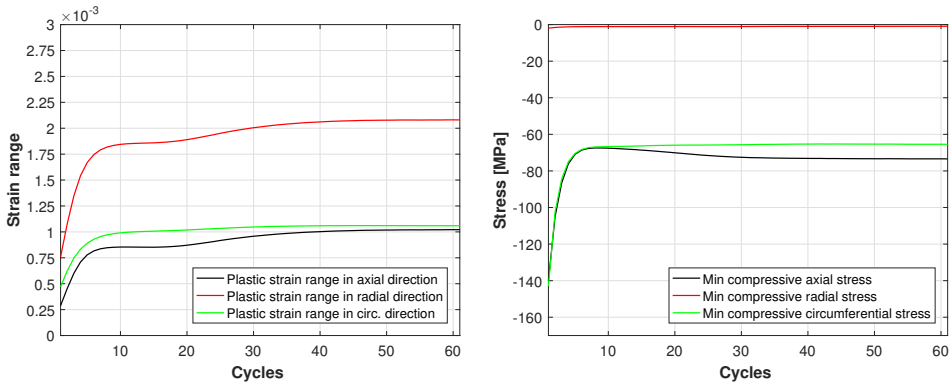

(a) (b)

Figure 3.26: Plastic strain range trend (a); Minimum compressive stress trend (b).

From the previous cases, in Figures contained in 3.26 the strain curves and stresses curve behave completely in different manner comparing with 3.20, 3.22, 3.24.
To conclude, stabilization is reached after 51 cycles but this model cannot be defined reliable.

3.5.4 Stabilized model

In this subsection another model is analyzed, it is the stabilized material model. This model was proposed by Chaboche in [4]. Briefly, it is a non- linear kinematic model that uses as values the material parameters when a material reaches stabilized conditions. In the end , this model neglects completely the initial state and takes into account young modulus, yield stress, from stabilized experimental stress-strain curves [3]; these data are presented in Table 3.11. Parameters C and γ are the same of the previous analyzed cases.

Temperature °C	σ_{0*} [MPa]	Es [GPa]
20	86	110.9
250	50	94.7
300	45	94.8

Table 3.11: Values of yield stress and elastic modulus used [3]

After some attempts to have a meaningful number of cycles, N = 20 is chosen. Results are depicted in Figures 3.27 and Figures 3.31.

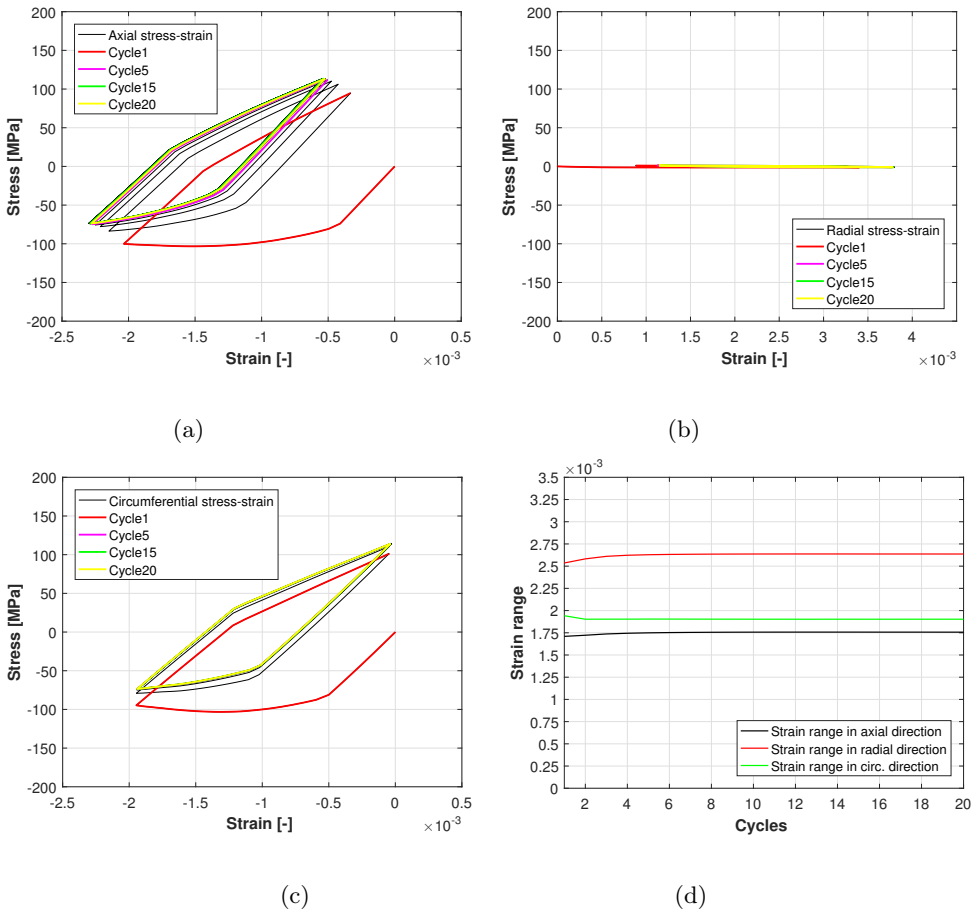

Figure 3.27: stress-strain curves for axial (a)radial (b) and circumferential direction (c), strain range curve (d).

From Figure 3.31 stabilization is reached after 11 cycles. The shape assumed is consistent with pure kinematic non linear model, but in order to have a clear vision a comparison is carried out in Figures 3.28a,3.27.

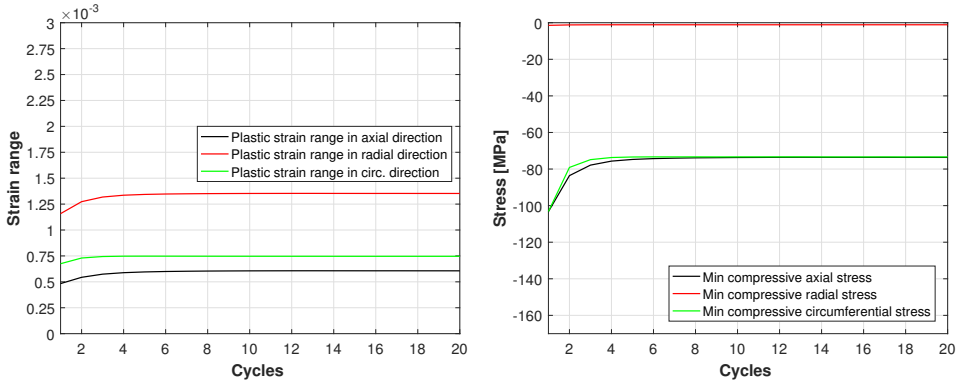

(a) (b)

Figure 3.28: Plastic strain range trend (a); Minimum compressive stress trend (b).

3.5.5 Linear kinematic model

The linear kinematic model is known as Prager's model. This one takes into consideration the initial conditions of the material, and assumes a linear function stress-strain after the yield stress. Due to this assumption the initial hardening modulus is the only parameter characteristic of the plastic region (Table 3.12). Data of such values are obtained from tensile tests at three levels [3]. Even in this case some attempts are required to find a reasonable number of cycles to reach stabilization.

Temperature °C	C [MPa]
20	37 439
250	18 039
300	18 466

Table 3.12: Linear kinematic material parameters used in the numerical simulation [3].

Finally a simulation is carried out for 5 cycles, Figures 3.29 demonstrates that they are enough, indeed in each case after three cycles the variation for

one cycle is under 0.01%. Particular attention is paid in the setting phase, since the solver has had lots of difficulties to reach convergence. To overcome this problem time step is set shorter and the maximum number of iterations is set grater in order to reach convergence; more details are in the Appendix. Moreover, the results comply with what was expected but the computational time is very large.

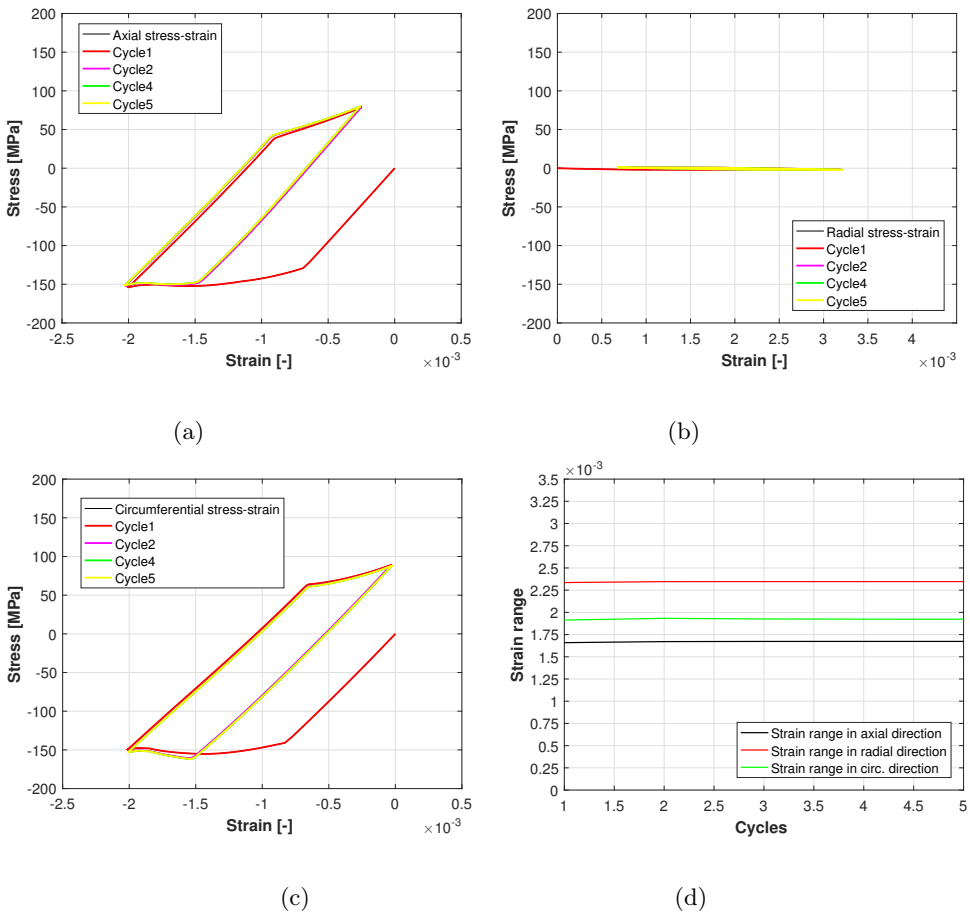

Figure 3.29: stress-strain curves for axial (a)radial (b) and circumferential direction (c), strain range curve (d).

In Figures 3.29 stabilization is reached; further investigations are needed to see how this model influences plastic strain range behavior .

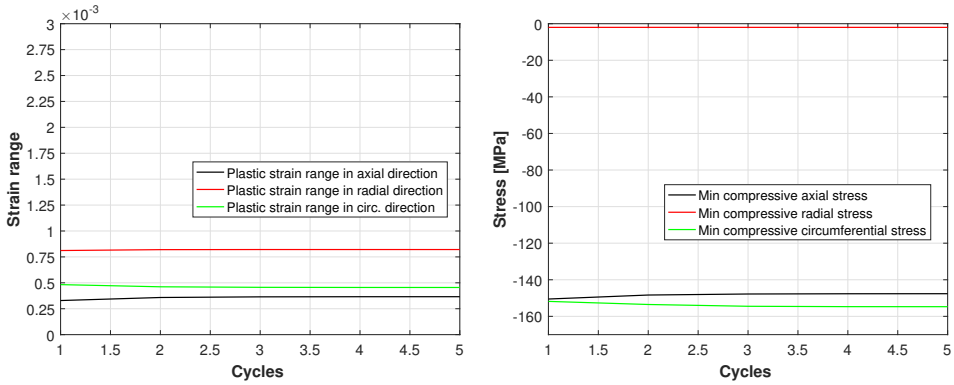

(a) (b)

Figure 3.30: Plastic strain range trend (a); Minimum compressive stress trend (b).

In Figures 3.30a and 3.30b the assumed behavior and the reached values are far from the combined model applied in the first case. There is a wide difference between axial and circumferential stresses in Figure 3.30b, and these values are much higher in compression, comparing with Figure 3.20b.
The purpose is now to understand if each model under-estimates or over-estimates the reference model analyzed in the beginning.
To conclude this section some meaningful graphs are plotted in Figure ??, 3.31b, 3.32.

In the abscissa N_n represents a normalized number of cycles: this value is obtained in any case, normalizing the number of cycles performed. In the ordinate the normalized plastic strain range, ε_{pl-n} is obtained by normalizing with respect to the last value of plastic strain range belonging to the combined model.

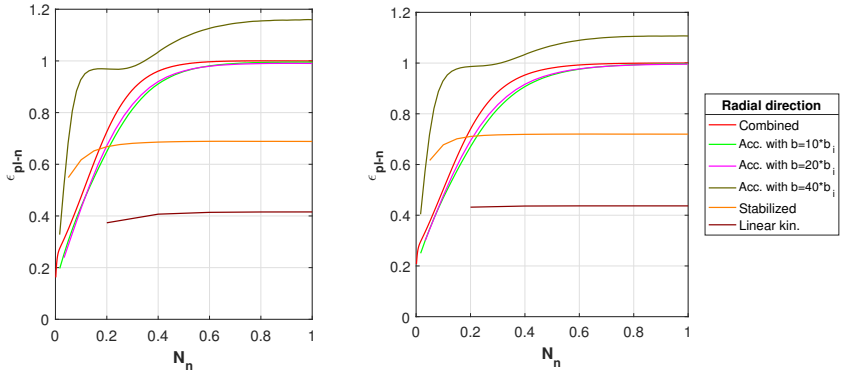

(a) (b)

Figure 3.31: Normalization of plastic strain range in axial direction (a), Normalization of plastic strain range in radial direction (b).

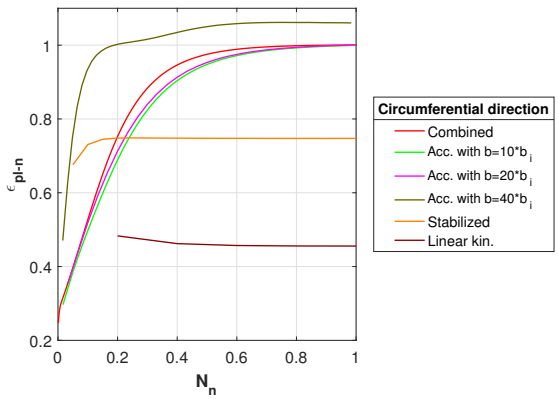

Figure 3.32: Normalization of plastic strain range in Circumferential direction.

3.6 Comparison of gathered results

At first sight a comparison between combined model, accelerated models, stabilized model and linear kinematic, shows slight and wide differences in the behavior of the plotted curves.
The purpose of this section is to compare some key factors; basically the minimum stresses achieved, the total strain range in the last cycle and the equivalent strain range. The equivalent strain range represents a value obtained

combining the three total strain ranges being in the presence of a multi-axial stress-strain state [18]. This value is represented by $\Delta\varepsilon_{eq}$ through equation (3.2) [18]; ε_2, ε_3, ε_1 give respectively axial, radial and circumferential total strain range, whereas the Δ afore represents the absolute difference [18].

$$\Delta\varepsilon_{eq} = \frac{\sqrt{2}}{3}\sqrt{[\Delta(\varepsilon_1 - \varepsilon_2)]^2 + [\Delta(\varepsilon_2 - \varepsilon_3)]^2 + [\Delta(\varepsilon_3 - \varepsilon_1)]^2} \tag{3.2}$$

In the Table 3.13 we present the results at the end of the first working condition.

Material model	Min S11 [MPa]	Δ_{S11} [%]	Min S22 [MPa]	Δ_{S22} [%]	Min S33 [MPa]	Δ_{S33} [%]
Combined	−156.7		−2.0		−152.5	
Acc. with $b = 10 * b_i$	−151.6	−3.3	−2.0	0	−151.7	−0.5
Acc. with $b = 20 * b_i$	−146.6	−6.4	−1.9	−10.0	−146.8	−3.7
Acc. with $b = 40 * b_i$	−139.9	−10.7	−1.9	−10.0	−142.9	−6.3
Stabilized	−103.3	−34.1	−1.4	−60.0	−103.2	−32.2
Linear kinematic	−150.2	−4.1	−2.0	0	−154.7	1.4

Table 3.13: Stress Comparison; S11=Axial stress, S22=Radial stress, S33=Circumferential stress, Δ_{sii} represents the relative error committed in each direction, taking as a reference the combined model.

In Table 3.13 minimum stress values are obtained from the first cycle due to softening stress decreases and total strain increases. This comparison is helpful to see how the first cycle changes and hence to have a rough idea about the variation arisen from combined model. Analyzing these values, in each case an underestimation is done; in cases where this value is in the range $\pm 5\%$ it can be considered acceptable.

The equivalent strain range can be assessed in every cycle, nevertheless in next chapter such value will be used when stabilized conditions are reached; so Tables 3.14 and 3.16 will present data linked with the last cycle performed. Table 3.14 presents strain data considering total strain, hence the sum of elastic and plastic strain.

Material model	ε_1 $*10^{-3}[-]$	$\mathtt{Err}_{11}$ %	ε_2 $*10^{-3}[-]$	$\mathtt{Err}_{22}$ %	ε_3 $*10^{-3}[-]$	$\mathtt{Err}_{33}$ %
Combined	1.79		2.89		1.91	
Acc. with $\mathtt{b} = 10 * \mathtt{b_i}$	1.84	+2.8	2.98	+3.1	1.97	+3.1
Acc. with $\mathtt{b} = 20 * \mathtt{b_i}$	1.77	+1.1	2.88	−0.3	1.92	+0.5
Acc. with $\mathtt{b} = 40 * \mathtt{b_i}$	1.97	+10.1	3.04	−5.2	1.90	−0.5
Stabilized	1.76	−1.7	2.64	−8.7	1.90	−0.5
Linear kinematic.	1.67	−6.7	2.35	−18.7	1.92	−0.5

Table 3.14: Strain range comparison for the last cycle computed; $\mathtt{Err}_{ii}$ represents the relative error committed in each direction, taking as a reference the combined model.

In Table 3.14 for case $\mathtt{b} = 10 * \mathtt{b_i}$ there is clear overestimation whereas for stabilized model and linear kinematic an underestimation occurs. Other considerations cannot be done without considering the equivalent strain range. It has been seen that considering the own stabilization criteria each model takes a certain number of cycles, so a summary is prepared in Table 3.15.

Material model	Number of cycles
Combined	349
Acc. model $\mathtt{b} = 10 * \mathtt{b_i}$	58
Acc. model $\mathtt{b} = 20 * \mathtt{b_i}$	28
Acc. model $\mathtt{b} = 40 * \mathtt{b_i}$	51
Stabilized	11
Linear kinematic	3

Table 3.15: Number of cycles to reach stabilization.

Material model	$\Delta\varepsilon_{\mathtt{eq}}$ $*10^{-3}$ [-]	$\mathtt{Err}_{\mathtt{eq}}$ [%]
Combined	3.16	
Acc. with $\mathtt{b} = 10 * \mathtt{b_i}$	3.16	−0.2
Acc. with $\mathtt{b} = 20 * \mathtt{b_i}$	3.15	−0.3
Acc. with $\mathtt{b} = 40 * \mathtt{b_i}$	3.31	+4.7
Stabilized	2.98	−5.7
Linear kinematic	2.77	−12.3

Table 3.16: Comparison of equivalent strain range; Eq.Sn=equivalent strain range; $\mathtt{Err}_{\mathtt{eq}}$ represents the relative error about the equivalent strain range committed in each direction, comparing with the combined model.

Now, some considerations can be done. Actually, in Table 3.16 only the accelerated model with $\mathtt{b} = 40 * \mathtt{b}$ overestimates the reference values, any other model underestimates the reference values determined with the combined model. Now is provided a comparison of the time employed by the solver to perform all the simulations computed.
The best solution is represented by a trade off between these concepts:

- Solution's reliability;
- Time employed;

The time employed for performing each simulation is given in the next table, together with the time to reach stabilization following the established criteria; this value is obtained by dividing the time employed for the number of cycles computed and multiplying for the number of cycles to reach stabilization (Table 3.15).

Material model	Time employed [s]	Cycles computed	Time to reach stabilization [s]
Combined	36 715	750	17 085
Acc. with $\mathtt{b} = 10 * \mathtt{b_i}$	2 266	60	2 577
Acc. with$\mathtt{b} = 20 * \mathtt{b_i}$	1 136	30	1060
Acc. with $\mathtt{b} = 40 * \mathtt{b_i}$	2 560	60	2 176
Stabilized	534	20	294
Linear kinematic	1 002	5	601

Table 3.17: Comparison of time employed to perform each simulation.

Chapter 4
Fatigue life

4.1 Introduction

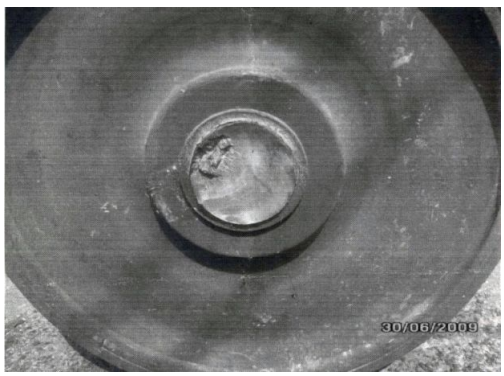

Figure 4.1: Railway axle broken (Viareggio accident) [19].

Component of machines, vehicles, and structures are frequently subject to repeated loadings, and the resulting cycling stresses can lead to microscopic physical damage to the material involved.
Even at stresses below the yield stress this microscopic damage can accumulate with continued cycling until it develops into a crack that leads to failure of the component. This phenomena of damage and failure due to cyclic loading is called fatigue [2]
In history this kind of breakdown has involved up to now lots of failures; for instance some some of the most notorious are the Comet plane, LOT Flight 7 etc. Hence Fatigue has been the subject of engineering efforts for more than 150 years when August Wholer studied and developed design strategies for avoiding fatigue failures of railway axles. An example is done from Figure 4.1

[19].
Generally, fatigue is split in two specified parts: high cycles fatigue (HCF) and low cycles fatigue (LCF). Low cycles fatigue occurs when during the cyclic loading the plastic deformation is dominant, so it is suggested to use the the 'strain-life approach' [2]. In the case belonging to HCF the stresses determine elastic behavior and hence a 'stress-life approach' is used. Due to the analysis performed in the previous chapter, in this study a strain based approach will be exploited [2][18].

4.2 Stress based approach and Strain based approach

As mentioned before, a stress based approach has to deal with HCF, but the main feature is the dependence from cyclic stresses. Working conditions could involve at the same time multi axial-stresses, hence an equivalent stress amplitude is evaluated and used to determine life through S-N curve [2]. Moreover, Basquin introduced the following formula to relates stress amplitude and lifetime [2].

$$\sigma_a = \sigma_f^{'}(2N_f)^{b^*} \tag{4.1}$$

where $\sigma_f^{'}$ is the fatigue strength coefficient, b^* is the fatigue strength exponent and N_f is the number of cycles to failure. Basically these coefficient are different for each material and they are determined with fatigue testing machines [20].
The strain based approach considers the plastic deformation that may occurs in localized regions where cracks begin. Stresses and strains in such regions are analyzed and used as basis for life estimation. The strain-based approach was initially developed in the late 1950 to analyze fatigue problems involving short fatigue life.
Figure 4.2 describes cyclic strain [3] [2].

Figure 4.2 considers a general case of loading through strain approach; the loading is sinusoidal and it is characterized by a mean value and an amplitude [2]. A maximum and a minimum value, respectively ε_{max} and ε_{min}, can be determined; some useful relations can be noticed [2]:

$$\Delta\varepsilon = \varepsilon_{max} - \varepsilon_{min} \tag{4.2}$$

$$\varepsilon_m = \frac{\varepsilon_{max} + \varepsilon_{min}}{2} \tag{4.3}$$

Equation (4.2) determines the strain range, while (4.3) gives the strain average; noticeable importance is covered by equation (4.5), which was developed independently in the mid 1950's from Manson and Coffin introducing the coefficients $\varepsilon_f^{'}$ and c known as fatigue ductility coefficient and fatigue ductility exponent.

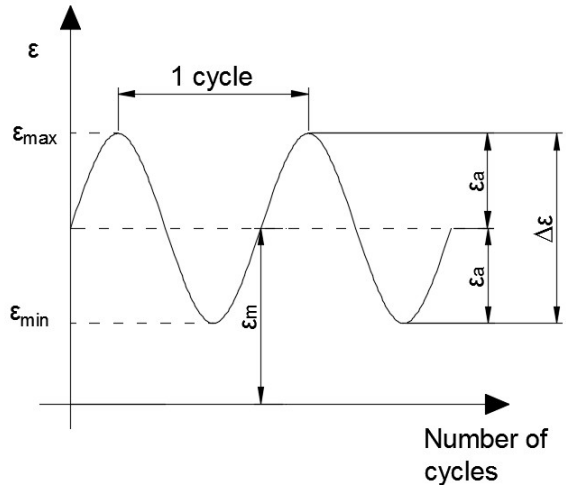

Figure 4.2: Strain time representation.

$$\Delta\varepsilon = \Delta\varepsilon_{el} + \Delta\varepsilon_{pl} \tag{4.4}$$

$$\frac{\Delta\varepsilon_{pl}}{2} = \varepsilon_f^{'}(2N_f)^c \tag{4.5}$$

$$\frac{\Delta\varepsilon_{el}}{2} = \frac{\sigma_f^{'}}{E}\left(2N_f\right)^{b^*} \tag{4.6}$$

In this study elastic and plastic strains occur, thus the basic equation (4.4) allows to determine the total strain range. Finally, combining equation (4.6) (obtained dividing equation (4.1)) with the Manson-Coffin (4.5) equation, the whole range of fatigue life is given by: (4.7)

$$\frac{\Delta\varepsilon}{2} = \left(\frac{2}{3}(1+\nu)\right)\frac{\sigma_f^{'}}{E}\left(2N_f\right)^{b^*} + \varepsilon_f^{'}(2N_f)^c \tag{4.7}$$

Before the determination of the service life in equation (4.7) a correction is suggested by Manson [10]: regarding the introduction of a coefficient for elastic part, this term is represented by

$$\frac{2}{3}(1+\nu) \tag{4.8}$$

In equation (4.7) the fatigue strength coefficient ($\sigma_f^{'}$), the fatigue strength exponent (b^*), the fatigue ductility coefficient ($\varepsilon_f^{'}$) and the fatigue ductility

exponent (c), are material dependent parameters; these values are even temperature dependent [3]. Due to working conditions these values are assessed at 300 °C [3]; such value are summarized in Table 4.1. Elastic modulus is kept for this temperature from Table 3.2.

Parameter	Value
$\sigma_f^{'}$ [MPa]	240.4
b^*	-0.1125
$\varepsilon_f^{'}$	0.5747
c	-0.6035

Table 4.1: Parameters for Manson-Coffin-Basquin equation assessed at 300 °C [3].

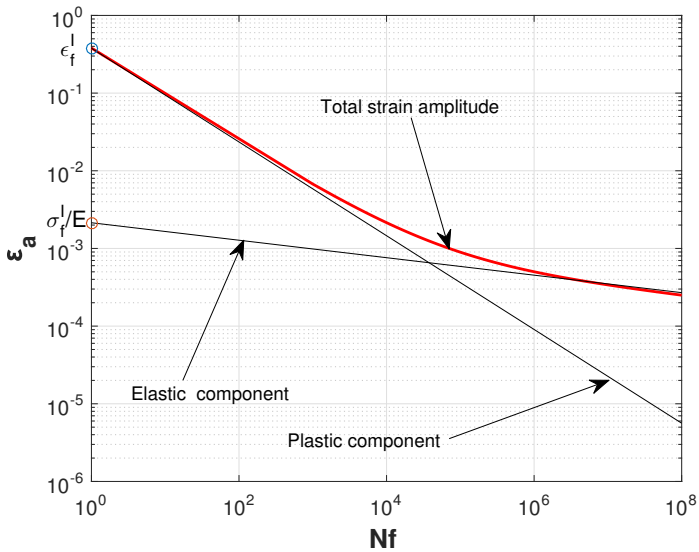

Figure 4.3: Manson-Coffin-Bausquin strain life curve.

4.3 Results concerning life estimation

At this point all factors needed to perform a service life assessment are available; Using formula 4.7

Material model	$\Delta\varepsilon_{eq}$ $*10^{-3}$	Life assessment [Cycles]	$\Delta\varepsilon_{rl}$ [%]
Combined	3.16	20 461	
Acc. with $b = 10 * b_i$	3.16	20 571	+0.5
Acc. with $b = 20 * b_i$	3.15	20 631	+0.8
Acc. with $b = 40 * b_i$	3.31	18 261	−10.8
Stabilized	2.98	23 791	+16.3
Linear kinematic	2.77	28 711	+40.3

Table 4.2: Number of cycles to failure estimation; $\Delta\varepsilon_{rl}$ = relative difference compared with combined model.

Thereby, getting Table 4.2 a judgement can be done. Only the accelerated model with $b = 40b_i$ gives an underestimation, so it should be the safest; however it has been shown in the previous chapter that this model is unreliable. Stabilized model and linear kinematic model overestimate in not-negligible manner the service life, so they can't be taken into consideration for design purposes. The accelerated model with $b = 10b_i$ and $b = 20b_i$ can be considered an optimal solutions, taking into account differences from the solution in the reference and the employed computational time; to conclude the best trade off is represented by the model that uses $b = 20b_i$.

Chapter 5
Conclusions

The goal of this work has been to investigate the behavior of a copper mold under cyclic thermal loads, giving an evaluation of fatigue life. This concept has been applied with different material models. Moreover, simulations were carried out using the Marc Mentat software belonging to Msc packages.
A copper mold for continuous casting represents the case study. For this reason chapter n. 3 provides a brief description about the main characteristics, employment and relative problems.
The first chapter discusses the theory of plasticity, and how it was developed into models, aiming to get a correspondence between real tests and numerical simulations. The most suitable models for cyclic behavior were identified. In chapter two several simulations on a simple specimen have been reported; such simulations were performed using both the Ansys and the Marc Mentat software. This part has been helpful to understand better how the material model behaves in the plastic domain (under cyclically loading), but also to capture the setting characteristics of software Marc Mentat. However the same results were obtained; the computational time employed by Marc Mentat was much shorter than the time employed by Ansys.
In this way, by using material data (with temperature dependence) coming from a previous study [3], a coupled thermal and mechanical analysis has been performed. Sensitivity analysis and simple tests were obviously needed in order to be sure of the obtained results. Subsequently simulations have analyzed a combined model, three accelerated model, the stabilized model and the linear kinematic model known as Prager's model. With accelerated models the computational time employed was strictly tied with the number of cycles to reach stabilization; such number has been determined using an empirical formula available in literature. Subsequently, Matlab allowed for a clear vision and comparison of the results obtained through graphs and tables.
The final step was related with the evaluation of fatigue life, but mostly it has shown how the computational amount of saved time can influence the obtained solution. In these cases a trade off is needed in order to balance computational

time and reliability of results. The last chapter has to deal with the assessment of fatigue life through the Manson-Coffin curve suited for the working conditions. The final comparison has shown that linear kinematic and stabilized models overestimate life duration in a non negligible manner; an accelerated model with speed of stabilization 40 times higher than the real value underestimates the life of about 11%, nevertheless such model is not useful because of the large distortion arising;the accelerated models with speed of stabilization 10 and 20 times higher than normal supply almost the same value of the combined model so the second one represents the best solution because it has taken the shortest computational time.

Appendix

Macro based on combined model using Marc Mentat; the commented part are marked with |

```
  *prog_analysis_class thermal/structural
  *set_model_length_unit meter    |unit of measure m;Kg,s,Celsius degrees
                  | point of the geometry
*add_points
0 0.100 0
0.050 0.100 0
0.200 0.100 0
0.500 0.100 0
1.000 0.100 0
0 0.116 0
0.050 0.116 0
0.200 0.116 0
0.500 0.116 0
1.000 0.116 0
                   | creation of surface
*add_surfaces  1 2 7 6 #
2 3 8 7 #
3 4 9 8  #
4 5 10 9 #
*fill_view

*set_convert_uvdiv u 23
*set_convert_uvdiv v 7
*convert_surfaces
all_selected 1  #

*set_convert_uvdiv u 140
*set_convert_uvdiv v  7
*convert_surfaces
```

```
all_selected  2 #

*set_convert_uvdiv u 210
*set_convert_uvdiv v 7
*convert_surfaces
all_selected 3  #

*set_convert_uvdiv u 180
*set_convert_uvdiv v 7
*convert_surfaces
all_selected  4 #

*sweep_nodes         | sweep of normal vectors of each element
all_existing

                  | tables defining the material properties

                           *new_md_table 1 1
                           *table_name el_mod
                          *set_md_table_type 1
                           temperature
                           *table_add
                           20 119.08e9
                           250 104e9
                           300 103e9     #

                           *new_md_table 1 1
                           *table_name yield_stress
                          *set_md_table_type 1
                           temperature
                           *table_add
                           20 130e6
                           250 111e6
                           300 110e6     #

                           *new_md_table 1 1
                           *table_name C
                          *set_md_table_type 1
                           temperature
                           *table_add
                           20 46250e6
                           250 45340e6
                           300 40080e6   #
```

```
                          *new_md_table 1 1
                          *table_name gamma
                         *set_md_table_type 1
                          temperature
                          *table_add
                          20 617.2
                          250 820.9
                          300 832.8   #

                          *new_md_table 1 1
                          *table_name r_inf
                         *set_md_table_type 1
                          temperature
                          *table_add
                          20 -75.7e6
                          250 -80.2e6
                          300 -76.6e6   #

    | with accelerated models value 1 is superimposes by 10
    |or 20 or 40 in this sentence :  *set_md_table_type 1

                          *new_md_table 1 1
                          *table_name b
                         *set_md_table_type 1
                          temperature
                          *table_add
                          20 2.352
                          250 3.894
                          300 5.293   #

      | imposition of axial-symmetry

              *new_geometry *geometry_type mech_axisym_solid
              *add_geometry_elements
              all_existing          #
              *new_mater standard *mater_option general:state:solid
              mater_option general:skip_structural:off

      | material properties settings

               @set($mat_prop_cdc,2)
               *mater_param general:mass_density 8930
               *mater_param structural:youngs_modulus 1
               *mater_param_table structural:youngs_modulus
```

```
          el_mod
          *mater_param structural:poissons_ratio 0.36

  *mater_option structural:plasticity:on
  *mater_option structural:plasticity_method:chaboche

*mater_param structural:yield_stress 1
 *mater_param_table structural:yield_stress
 yield_stress

    *mater_param structural:chaboche_rinf 1
    *mater_param_table structural:chaboche_rinf
    r_inf

           *mater_param structural:chaboche_b 1
           *mater_param_table structural:chaboche_b
           b

         *mater_param structural:chaboche_c 1
         *mater_param_table structural:chaboche_c
         C

        *mater_param structural:chaboche_gamma 1
        *mater_param_table structural:chaboche_gamma
        gamma

         *mater_option thermal:mass_density:thermal
         *mater_param thermal:mass_density 8900
         *mater_option structural:thermal_expansion:on
         *mater_param structural:thermal_exp 17e-6

  @set($mat_prop_cdc,3)
  *mater_param thermal:conductivity 390
  *mater_param thermal:specific_heat 385
  *mater_param thermal:ref_temp_enth_formation 20

                        *add_mater_elements
                        all_existing  #

    | initial condition
                  *new_icond *icond_type temperature
                  *icond_dof_value t1 20
                  *add_icond_nodes
                  all_existing    #
```

```
      | mechanical boundary conditions

        *new_apply *apply_type fixed_displacement
         *apply_dof x *apply_dof_value x
         *add_apply_nodes   2562   #

       | definition of thermal flux used

 *new_md_table 1 1
x0_coordinate
*edit_table table_flu
x0_coordinate
*table_add
0.000000000 0.000000              |thermal flux profile
0.100000000 0.000000
0.100443459 0.197039
0.10275314 0.399267
0.10413895 0.700702
     :        :
     :        :
0.978277 1.24634
0.98713 1.2209
0.99329 1.205
0.999834 1.21136
 #

*edit_table table1
*set_md_table_type 1
x0_coordinate
*edit_table table1 *table_name
Thermal_flux

       | thermal boundary conditions

              *new_apply *apply_type edge_flux
*apply_name Heat_lux
*apply_dof q
*apply_dof_value q 1.6e6         | heat flux corrected
*apply_dof_table q
Thermal_flux

*add_apply_edges
 1:0 2:0 3:0 4:0 5:0 6:0 7:0 8:0 ......  #
```

```
*new_apply *apply_type edge_film
*apply_name convenction_h20
*apply_dof h
*apply_param_value temp_inf 40
*apply_dof_value h 48000    | w/(m2*k)
*add_apply_edges
139:2 140:2 141:2 14270:2 3871:2 ..........  #


             |  loadcase settings

               *new_loadcase *loadcase_type therm/struc:trans/static
               *loadcase_value time 30
               *edit_apply Heat_lux
               *loadcase_name heating

               *loadcase_option stepping:multicriteria
               *loadcase_value maxfraction 0.05

            *new_loadcase *loadcase_type therm/struc:trans/static
            *loadcase_name cooling
            *remove_loadcase_loads Heat_lux
            *loadcase_value time 30

           *loadcase_option stepping:multicriteria
           *loadcase_value maxfraction 0.05


*edit_loadcase heating *copy_loadcase
  *edit_loadcase lcase3 *loadcase_name    h2
 *edit_loadcase cooling *copy_loadcase
  *edit_loadcase lcase4 *loadcase_name    c2


 *edit_loadcase heating *copy_loadcase
  *edit_loadcase lcase5 *loadcase_name    h3
 *edit_loadcase cooling *copy_loadcase
  *edit_loadcase lcase6 *loadcase_name    c3

          :
          :

 *edit_loadcase heating *copy_loadcase
```

```
 *edit_loadcase lcase239 *loadcase_name    h770
*edit_loadcase cooling *copy_loadcase
 *edit_loadcase lcase240 *loadcase_name    c770


       | definition of the whole simulation

  *prog_use_current_job on *new_job *job_class thermal/structural
  *add_job_loadcases heating
  *add_job_loadcases cooling


         *add_job_loadcases h2
 *add_job_loadcases c2
 *add_job_loadcases h3
 :
 :
 *add_job_loadcases c770
  *add_job_loadcases h770

     |definition of results required

            *job_option dimen:axisym
             *add_post_tensor stress
             *add_post_tensor el_strain
             *add_post_tensor pl_strain


@set($eltypecmd,*element_type) @set($eltypename,ELEMENT TYPES)
@set($threed_anl_dim,false) @set($axisym_anl_dim,true)

 @set($planar_anl_dim,false)
*element_type 28
all_existing

           | imposition of large strain

            *edit_job job2
            *job_option strain:large

          *job_option large_strn_proc:upd_lagrange

           *job_option post_int_points:centroid
```

```
            | gpu and number of threads settings

           *update_job
           *job_option assem_recov_multi_threading:on
           *job_option mfront_sparse_multi_threading:on
           *job_option solver_use_gpu:on
           *job_param assem_recov_nthreads 8
           *job_param nthreads 8
           *submit_job 1 *monitor_job
```

The follow macro is used to perform linear stabilized model model.

```
*prog_analysis_class thermal/structural
*set_model_length_unit meter    |unit of measure m;Kg,s,Celsius degrees


*add_points
0 0.100 0
0.050 0.100 0
0.200 0.100 0
0.500 0.100 0
1.000 0.100 0
0 0.116 0
0.050 0.116 0
0.200 0.116 0
0.500 0.116 0
1.000 0.116 0

*add_surfaces  1 2 7 6 #
2 3 8 7 #
3 4 9 8  #
4 5 10 9 #
*fill_view

*set_convert_uvdiv u 23
*set_convert_uvdiv v 7
*convert_surfaces
all_selected 1  #

*set_convert_uvdiv u 140
*set_convert_uvdiv v  7
*convert_surfaces
all_selected  2 #

*set_convert_uvdiv u 210
```

```
*set_convert_uvdiv v 7
*convert_surfaces
all_selected 3  #


*set_convert_uvdiv u 180
*set_convert_uvdiv v 7
*convert_surfaces
all_selected  4 #

*sweep_nodes
all_existing
    *new_md_table 1 1
                              *table_name el_mod
                             *set_md_table_type 1
                              temperature
                              *table_add
                              20 110.9e9
                              250 94.7e9
                              300 94.8e9     #

                              *new_md_table 1 1
                              *table_name yield_stress
                             *set_md_table_type 1
                              temperature
                              *table_add
                              20 86e6
                              250 50e6
                              300 45e6     #

                              *new_md_table 1 1
                              *table_name C
                             *set_md_table_type 1
                              temperature
                              *table_add
                              20 46250e6
                              250 45340e6
                              300 40080e6   #

                              *new_md_table 1 1
                              *table_name gamma
                             *set_md_table_type 1
                              temperature
                              *table_add
```

```
                        20 617.2
                        250 820.9
                        300 832.8   #

                        *new_md_table 1 1
                        *table_name r_inf
                       *set_md_table_type 1
                        temperature
                        *table_add
                        20 -75.7e6
                        250 -80.2e6
                        300 -76.6e6   #

                        *new_md_table 1 1
                        *table_name b
                       *set_md_table_type 1
                        temperature
                        *table_add
                        20 2.352
                        250 3.894
                        300 5.293   #


    *new_geometry *geometry_type mech_axisym_solid
    *add_geometry_elements
    all_existing          #
    *new_mater standard *mater_option general:state:solid
    *mater_option general:skip_structural:off
    @set($mat_prop_cdc,2)
    *mater_param general:mass_density 8930
    *mater_param structural:youngs_modulus 1
    *mater_param_table structural:youngs_modulus
    el_mod
    *mater_param structural:poissons_ratio 0.36

*mater_option structural:plasticity:on
*mater_option structural:plasticity_method:chaboche

*mater_param structural:yield_stress 1
*mater_param_table structural:yield_stress
yield_stress

                *mater_param structural:chaboche_rinf 0
               | *mater_param_table structural:chaboche_rinf
```

```
                          | r_inf


                           *mater_param structural:chaboche_b 0
                          |   *mater_param_table structural:chaboche_b
                          |   b

                            *mater_param structural:chaboche_c 1
                             *mater_param_table structural:chaboche_c
                              C

                            *mater_param structural:chaboche_gamma 1
                            *mater_param_table structural:chaboche_gamma
                             gamma

              *mater_option thermal:mass_density:thermal
              *mater_param thermal:mass_density 8900
              *mater_option structural:thermal_expansion:on
              *mater_param structural:thermal_exp 17e-6

           @set($mat_prop_cdc,3)
           *mater_param thermal:conductivity 390
           *mater_param thermal:specific_heat 385
           *mater_param thermal:ref_temp_enth_formation 20

                                *add_mater_elements
                                all_existing  #



             *new_icond *icond_type temperature
             *icond_dof_value t1 20
             *add_icond_nodes
             all_existing    #

          *new_apply *apply_type fixed_displacement
          *apply_dof x *apply_dof_value x
         *add_apply_nodes   2562   #

 *new_md_table 1 1
x0_coordinate
*edit_table table_flu
x0_coordinate
*table_add
```

```
0.000000000 0.000000
0.100000000 0.000000
0.100443459 0.197039
0.10275314 0.399267
:
:
:
0.978277 1.24634
0.98713 1.2209
0.99329 1.205
0.999834 1.21136
 #

*edit_table table1
*set_md_table_type 1
x0_coordinate
*edit_table table1 *table_name
Thermal_flux


*new_apply *apply_type edge_flux
*apply_name Heat_lux
*apply_dof q
*apply_dof_value q 1.6e6
*apply_dof_table q
Thermal_flux

*add_apply_edges
 1:0 2:0 3:0 4:0 5:0 6:0 7:0 8:0 ............. #

*new_apply *apply_type edge_film
*apply_name convenction_h20
*apply_dof h
*apply_param_value temp_inf 40
*apply_dof_value h 48000    | w/(m2*k)
*add_apply_edges
139:2 140:2 141:2 142:2 143:2 144:2 .........  #


          *new_loadcase *loadcase_type therm/struc:trans/static
          *loadcase_value time 30
          *edit_apply Heat_lux
          *loadcase_name heating
```

```
         *loadcase_option stepping:multicriteria
         *loadcase_value maxfraction 0.05




            *new_loadcase *loadcase_type therm/struc:trans/static
            *loadcase_name cooling
            *remove_loadcase_loads Heat_lux
            *loadcase_value time 30

     *loadcase_option stepping:multicriteria
     *loadcase_value maxfraction 0.05

*edit_loadcase heating *copy_loadcase
  *edit_loadcase lcase3 *loadcase_name    h2
 *edit_loadcase cooling *copy_loadcase
  *edit_loadcase lcase4 *loadcase_name    c2


 *edit_loadcase heating *copy_loadcase
  *edit_loadcase lcase5 *loadcase_name    h3
 *edit_loadcase cooling *copy_loadcase
  *edit_loadcase lcase6 *loadcase_name    c3
 :
 :
 :
 *edit_loadcase heating *copy_loadcase
  *edit_loadcase lcase263 *loadcase_name    h20
 *edit_loadcase cooling *copy_loadcase
  *edit_loadcase lcase264 *loadcase_name    c20

     *prog_use_current_job on *new_job *job_class thermal/structural
     *add_job_loadcases heating
     *add_job_loadcases cooling
     *job_option dimen:axisym

               *add_post_tensor stress
               *add_post_tensor stress_g
               *add_post_tensor cauchy
               *add_post_var temperature
               *add_post_var von_mises

      *prog_use_current_job on *new_job *job_class thermal/structural
```

```
      *add_job_loadcases heating
      *add_job_loadcases cooling

  *add_job_loadcases h2
  *add_job_loadcases c2
  ;
  *add_job_loadcases h130
  *add_job_loadcases c130

               *job_option dimen:axisym
                *add_post_tensor stress
                *add_post_tensor el_strain
                *add_post_tensor pl_strain

  @set($eltypecmd,*element_type) @set($eltypename,ELEMENT TYPES)
  @set($threed_anl_dim,false) @set($axisym_anl_dim,true)
   @set($planar_anl_dim,false)
              *element_type 28
              all_existing

              *edit_job job2
              *job_option strain:large

            *job_option large_strn_proc:upd_lagrange
             *job_option post_int_points:centroid

              *update_job
              *job_option assem_recov_multi_threading:on
              *job_option mfront_sparse_multi_threading:on
             *job_option solver_use_gpu:on
             *job_param assem_recov_nthreads 8
             *job_param nthreads 8
```

The follow macro is used to perform linear kinematic model.

```
*prog_analysis_class thermal/structural
*set_model_length_unit meter    |unit of measure m;Kg,s,Celsius degrees


*add_points
0 0.100 0
0.050 0.100 0
0.200 0.100 0
0.500 0.100 0
1.000 0.100 0
```

```
0 0.116 0
0.050 0.116 0
0.200 0.116 0
0.500 0.116 0
1.000 0.116 0

*add_surfaces  1 2 7 6 #
2 3 8 7 #
3 4 9 8  #
4 5 10 9 #
*fill_view

*set_convert_uvdiv u 23
*set_convert_uvdiv v 7
*convert_surfaces
all_selected 1  #


*set_convert_uvdiv u 140
*set_convert_uvdiv v  7
*convert_surfaces
all_selected  2 #

*set_convert_uvdiv u 210
*set_convert_uvdiv v 7
*convert_surfaces
all_selected 3  #


*set_convert_uvdiv u 180
*set_convert_uvdiv v 7
*convert_surfaces
all_selected  4 #

*sweep_nodes
all_existing
                            *new_md_table 1 1
                            *table_name el_mod
                           *set_md_table_type 1
                            temperature
                            *table_add
                            20 119.08e9
                            250 104e9
                            300 103e9     #
```

```
 *new_md_table 1 1
 *table_name yield_stress
*set_md_table_type 1
 temperature
 *table_add
 20 130e6
 250 111e6
 300 110e6     #

 *new_md_table 1 1
 *table_name C
*set_md_table_type 1
 temperature
 *table_add
 20 37439e6
 250 18039e6
 300 18466e6   #

 *new_md_table 1 1
 *table_name gamma
*set_md_table_type 1
 temperature
 *table_add
 20 617.2
 250 820.9
 300 832.8   #

 *new_md_table 1 1
 *table_name r_inf
*set_md_table_type 1
 temperature
 *table_add
 20 -75.7e6
 250 -80.2e6
 300 -76.6e6   #

 *new_md_table 1 1
 *table_name b
*set_md_table_type 1
 temperature
 *table_add
 20 2.352
 250 3.894
```

```
                                300 5.293   #


*new_md_table 2 1
*table_name yield_stress1
*set_md_table_type 1
temperature
@set($civ,2) @set($iv1bool,false) @set($iv2bool,true) @set($iv3bool,false)
@set($iv4bool,false)
*set_md_table_type 2
eq_plastic_strain
*md_table_add_all
3
2
20
250
300
0
0.5
1
0.8538462
0.84615384
144.996
70.2346
71.86

                 *new_geometry *geometry_type mech_axisym_solid
                 *add_geometry_elements
                 all_existing          #
                 *new_mater standard *mater_option general:state:solid
                 *mater_option general:skip_structural:off
                 @set($mat_prop_cdc,2)
                 *mater_param general:mass_density 8930
                 *mater_param structural:youngs_modulus 1
                 *mater_param_table structural:youngs_modulus
                 el_mod
                 *mater_param structural:poissons_ratio 0.36

                 *mater_option structural:plasticity:on
                 *mater_option structural:plasticity_method:table

                *mater_option structural:hardening_rule:kinematic
                *mater_param structural:yield_stress 130e6
```

```
              *mater_param structural:yield_stress 130e6
              *mater_param_table structural:yield_stress
              yield_stress1

            *mater_option thermal:mass_density:thermal
            *mater_param thermal:mass_density 8900
            *mater_option structural:thermal_expansion:on
            *mater_param structural:thermal_exp 17e-6

    @set($mat_prop_cdc,3)
    *mater_param thermal:conductivity 390
    *mater_param thermal:specific_heat 385
    *mater_param thermal:ref_temp_enth_formation 20

                                *add_mater_elements
                                all_existing  #



          *new_icond *icond_type temperature
          *icond_dof_value t1 20
          *add_icond_nodes
          all_existing    #

        *new_apply *apply_type fixed_displacement
        *apply_dof x *apply_dof_value x
        *add_apply_nodes   2562   #


 *new_md_table 1 1
x0_coordinate
*edit_table table_flu
x0_coordinate
*table_add
0.000000000 0.000000
0.100000000 0.000000
0.100443459 0.197039
0.10275314 0.399267
:
:
:
0.98713 1.2209
```

```
0.99329 1.205
0.999834 1.21136
 #

*edit_table table1
*set_md_table_type 1
x0_coordinate
*edit_table table1 *table_name
Thermal_flux


              *new_apply *apply_type edge_flux
*apply_name Heat_lux
*apply_dof q
*apply_dof_value q 1.6e6
*apply_dof_table q
Thermal_flux

*add_apply_edges
 1:0 2:0 3:0 4:0 5:0 6:0 7:0 ................ #

*new_apply *apply_type edge_film
*apply_name convenction_h20
*apply_dof h
*apply_param_value temp_inf 40
*apply_dof_value h 48000    | w/(m2*k)
*add_apply_edges
139:2 140:2 141:2 142:2 143:2 144:2 145:2 ..........   #


        *new_loadcase *loadcase_type therm/struc:trans/static
        *loadcase_value time 30
        *edit_apply Heat_lux
        *loadcase_name heating

            *loadcase_value nsteps 150
            *loadcase_option stepping:multicriteria
            *loadcase_value maxfraction 0.005

            *edit_loadcase heating
            *loadcase_value desired 100
            *loadcase_value scale_step 1.07

        *new_loadcase *loadcase_type therm/struc:trans/static
```

```
        *loadcase_name cooling
        *remove_loadcase_loads Heat_lux
        *loadcase_value time 30


       *loadcase_value nsteps 150
       *loadcase_option stepping:multicriteria
       *loadcase_value maxfraction 0.005

      *edit_loadcase cooling
      *loadcase_value desired 100
      *loadcase_value scale_step 1.1


*edit_loadcase heating *copy_loadcase
  *edit_loadcase lcase3 *loadcase_name    h2
 *edit_loadcase cooling *copy_loadcase
  *edit_loadcase lcase4 *loadcase_name    c2


 *edit_loadcase heating *copy_loadcase
  *edit_loadcase lcase5 *loadcase_name    h3
 *edit_loadcase cooling *copy_loadcase
  *edit_loadcase lcase6 *loadcase_name    c3


 *edit_loadcase heating *copy_loadcase
  *edit_loadcase lcase7 *loadcase_name    h4
 *edit_loadcase cooling *copy_loadcase
  *edit_loadcase lcase8 *loadcase_name    c4


 *edit_loadcase heating *copy_loadcase
  *edit_loadcase lcase9 *loadcase_name    h5
 *edit_loadcase cooling *copy_loadcase
  *edit_loadcase lcase10 *loadcase_name    c5


*prog_use_current_job on *new_job *job_class thermal/structural
*add_job_loadcases heating
*add_job_loadcases cooling
*add_job_loadcases h2
*add_job_loadcases c2
*add_job_loadcases h3
```

```
*add_job_loadcases c3
*add_job_loadcases h4
*add_job_loadcases c4
*add_job_loadcases h5
*add_job_loadcases c5
  *job_option dimen:axisym

           *add_post_tensor stress
           *add_post_tensor stress_g
           *add_post_tensor cauchy
           *add_post_var temperature
           *add_post_var von_mises


   *prog_use_current_job on *new_job *job_class thermal/structural
   *add_job_loadcases heating
   *add_job_loadcases cooling

 *add_job_loadcases h2

      *job_option dimen:axisym
      *add_post_tensor stress
      *add_post_tensor el_strain
      *add_post_tensor pl_strain



@set($eltypecmd,*element_type) @set($eltypename,ELEMENT TYPES)
@set($threed_anl_dim,false) @set($axisym_anl_dim,true)
 @set($planar_anl_dim,false)
*element_type 28
 all_existing

              *edit_job job2
              *job_option strain:large

      *job_option large_strn_proc:upd_lagrange


         *job_option post_int_points:centroid

                *update_job
                *job_option assem_recov_multi_threading:on
                *job_option mfront_sparse_multi_threading:on
```

```
*job_option solver_use_gpu:on
*job_param assem_recov_nthreads 8
*job_param nthreads 8
*submit_job 1 *monitor_job
```

References

[1] Lemaitre, Jean, and Jean-Louis Chaboche. Mechanics of solid materials. Cambridge university press, 1994. (Cited on pages 1, 2, 3, 5, 6, 8, 9, 10, 11, 12, and 38.)

[2] Lee, Yung-Li, Mark E. Barkey, and Hong-Tae Kang. Metal fatigue analysis handbook: practical problem-solving techniques for computer-aided engineering. Elsevier, 2011. (Cited on pages 3, 4, 5, 6, 7, 8, 9, 10, 11, 57, and 58.)

[3] Jelena Srnec Novak, Denis Benasciutti. Parameter estimation of cyclic plasticity models and strain based fatigues curves in numerical analysis of mechanical components under thermal loads. (Cited on pages i, xi, 3, 5, 6, 7, 9, 10, 11, 12, 15, 27, 34, 47, 48, 49, 58, 60, and 63.)

[4] Chaboche, J. L. "A review of some plasticity and viscoplasticity constitutive theories." International Journal of Plasticity 24.10 (2008): 1642-1693. (Cited on pages 12 and 47.)

[5] ASTM International: tensile Testing, second edition,2004 (Not cited.)

[6] `http://ietd.iipnetwork.org/content/continuous-casting` (Cited on pages viii and 25.)

[7] Stephens, Ralph I., et al. Metal fatigue in engineering. John Wiley, Sons, 2000. (Not cited.)

[8] `https://www.sharcnet.ca/Software/Ansys/16.2.3/en-us/help/ans_elem/Hlp_E_PLANE183.html` (Cited on page 15.)

[9] `https://www.zwickroell.it/it/applicazioni/plastica/materiali-termoplastici-e-termoindurenti/prove-di-trazione-su-plastiche.html` (Cited on page 3.)

[10] Manson, S. S., and G. R. Halford. "Fatigue and durability of metals at high temperature, 2nd edn, Chapter 7." ASM International, Materials Park, OH, Printed in the United States of America (2009). (Cited on pages 6 and 59.)

[11] Meng, Y. A., and Brian G. Thomas. "Heat-transfer and solidification model of continuous slab casting: CON1D." Metallurgical and Materials Transactions B 34.5 (2003): 685-705. (Not cited.)

[12] Mahapatra, R. B., et al. "Mold behavior and its influence on quality in the continuous casting of steel slabs: Part i. Industrial trials, mold temperature measurements, and mathematical modeling." Metallurgical Transactions B 22.6 (1991): 861-874. (Cited on pages 25, 26, and 34.)

[13] Mahapatra, R. B., J. K. Brimacombe, and I. V. Samarasekera. "Mold behavior and its influence on quality in the continuous casting of steel slabs: Part II. Mold heat transfer, mold flux behavior, formation of oscillation marks, longitudinal off-corner depressions, and subsurface cracks." Metallurgical Transactions B 22.6 (1991): 875-888. (Cited on pages 25, 26, and 34.)

[14] GALDIZ, PAUL, et al. "ROUND CONTINUOUS CASTING WITH EMS-CFD COUPLED." APA (Cited on pages xi, 26, 27, 29, and 31.)

[15] Marc 2015 Volume A: Element Library. Msc software. (Not cited.)

[16] Marc 2015 Volume B: Theory and user information. Msc software. (Cited on page 28.)

[17] Park, Joong Kil, et al. "Thermal and mechanical behavior of copper molds during thin-slab casting (II): Mold crack formation." Metallurgical and Materials Transactions B 33.3 (2002): 437-449. (Not cited.)

[18] Manson, Samuel Stanford. "Thermal stress and low-cycle fatigue." (1966). APA (Cited on pages 53 and 58.)

[19] http://www.americaoggi.info/2009/07/02/13091-strage-di-viareggio-forse-un-asse-del-treno-fessurato-e-parzialmente-corroso (Cited on pages ix, 57, and 58.)

[20] http://www.finegrouptest.com/digital-fatigue-testing-machine.html (Cited on page 58.)